Summer 8-2015

Process and Reactor Level Simulations of Calcium Looping Combustion

Wei Dai
Washington University in St. Louis

WASHINGTON UNIVERSITY IN ST. LOUIS

School of Engineering and Applied Science

Department of Mechanical Engineering and Material Science

Thesis Examination Committee:
Ramesh K. Agarwal, Chair
David A. Peters
Michael Wendl

Process and Reactor Level Simulations of Calcium Looping Combustion

by

Wei Dai

A thesis presented to the School of Engineering and Applied Science
of Washington University in St. Louis in partial fulfillment of the
requirements for the degree of
Master of Science

August 2015

Saint Louis, Missouri

Contents

List of Figures

List of Tables

Acknowledgments

I would like to thank Dr. Ramesh Agarwal, my thesis advisor, for his continuous help and encouragement on research reported in this thesis. I would also like to thank the thesis examining committee members, Dr. David Peters and Dr. Michael Wendl, for spending time in reading the thesis and offering constructive suggestions. I would like to thank Subhodeep Banerjee for his helpful guidance, discussions and suggestions at every step of my research. Thanks also to Xiao Zhang for sharing his knowledge and experience. Finally I appreciate all the support provided by the colleagues in the CFD laboratory of the department of Mechanical Engineering and Material Science.

Wei Dai

Washington University in St. Louis
August 2015

Dedication

Dedicated to Yi Wang, Minqiang Dai and Yufei.

ABSTRACT OF THE THESIS

Process and Reactor Level Simulations
of Calcium Looping Combustion
by

Wei Dai

Master of Science in Mechanical Engineering

Washington University in St. Louis, 2015

Research Advisor: Professor Ramesh K. Agarwal

Calcium looping (CaL) is a recent technology for carbon capture from coal fired power plants which consumes less energy than other approaches such as oxy-fuel. In the first part of this thesis, a system level model is developed in ASPEN PLUS to calculate the energy penalty of introducing Calcium looping in a coal fired power plant. Several simplifications and assumptions are made to model the Calcium looping process. The relationship between the energy penalty due to CaL and carbon capture efficiency is used to validate the process model for both pre-combustion CaL and post-combustion CaL; it agrees well with the experimental data and simulation results available in the literature. The simulation shows an increasing marginal energy penalty associated with an increase in the carbon capture efficiency, which limits the maximum carbon capture efficiency to around 95-98% before the energy penalty becomes too large. In the second part of the thesis, a reactor level model is built using ANSYS FLUENT to perform a CFD simulation of a fluidized bed where the carbonation reaction (one of the two major reactions in CaL) takes place. Both planar and axi-symmetry models of the reactor are considered and the carbon capture efficiency is evaluated for various combinations of the velocity and CO_2 mole fraction at inlet of the reactor. It is found that reducing the inlet velocity has a significant impact on the carbon capture efficiency by increasing the

residual time of the gases inside the reactor. Based on these results, the relative merit of Calcium looping versus Chemical Looping Combustion is examined.

Chapter 1 Introduction

1.1 Background Information

It is well established that Carbon-dioxide is a major cause for greenhouse effect. The release of CO_2 in atmosphere primarily comes from burning of fossil fuels. Carbon capture is a technology deployed for capturing CO_2 from large-scale point sources, such as fossil fuel power plants, steel and cement factories among others. Calcium looping (CaL) is one of the carbon capture technology which utilizes calcium-oxide (CaO) as sorbent to capture CO_2.

Calcium looping is basically a loop of chemical reactions consisting of two major types: one for capture of CO_2 (called carbonation), and the other for release of CO_2 (called calcination) in two interconnected reactors. Each reaction is a reverse of the other reaction. The conceptual setup includes two major reactors called the carbonator and the calciner in which the two chemical reactions takes place. When the flue gas enters the carbonator, CO_2 is captured by CaO to form calcium-carbonate ($CaCO_3$). A stream of CO_2-lean flue gas then comes out of the carbonator. After nearly all CaO in carbonator converts into $CaCO_3$, the solid $CaCO_3$ is transported to the other reactor--the calciner where $CaCO_3$ is heated to break into CaO and CO_2 again. The CaO from calciner is then transported back to carbonator and the stream of pure CO_2 from calciner is then sent for pressurized storage.

The goal of Calcium looping is to consume the least amount of energy to achieve high CO_2 capture efficiency. Therefore the estimation of the energy penalty in CaL and the efficient design of the reactors are of great interest in the field of Calcium looping Combustion.

1.2 Motivation

Energy penalty (for employing CaL in a power plant) is a term referred to the portion of energy consumed by CaL from the total generated by a power plant. It is a measure of the performance of a CaL system. In this thesis, simple models of CaL are created to calculate the energy penalty in a CaL system. Two main types of CaL systems are studied -- the post-combustion capture and pre-combustion capture system. The performance of these systems is studied and compared.

In addition to the macro-scale calculations of energy penalty using ASPEN Plus modeling software, some reactor-level simulations are also conducted using the CFD software ANSYS FLUENT. Employing simplified reactor setups, the simulations are conducted to obtain some basic information on reactor-level flow and influence of reactor shape. Inflow conditions are varied and their influence is examined.

Chapter 2 Analysis Tools

2.1 Introduction to ASPEN PLUS

ASPEN PLUS is a chemical process optimization software developed by AspenTech, Inc. Its user can define a series of chemical reactions related to each other, with blocks and streams of various capabilities (i.e. the reactor block and material stream). In addition, more specific properties of processes and reactions can be established within the blocks and streams. It also provides the sensitivity analysis tool and an optimization tool, which allow users to examine how some outcome is influenced by some inputs, and to optimize some variables to achieve specific goals with acceptable constraints.

In this thesis, ASPEN is simplified for simulating the chemical reactions involved in CaL, and to determine how the energy penalty varies with change in carbon-capture efficiency.

2.2 Introduction to ANSYS FLUENT

ANSYS FLUENT is a fluid simulation software based on the principles of Computational Fluid Dynamics (CFD). It is currently owned by ANSYS, Inc. FLUENT can simulate complex flows including the effects of turbulence, heat transfer, and chemical reactions. FLUENT is widely used in industry and academic research.

FLUENT is employed in this thesis to model a multiphase flow with reaction in the carbonation reactor.

Chapter 3 Process Level Simulations

There are in general two kinds of Calcium looping technology: post-combustion capture and pre-combustion capture. Post-combustion capture is a technology that includes Calcium looping at the end of combustion process; thus the CO_2 in the flue gas generated due to combustion is captured. Pre-combustion capture is a technology that substantially changes the process of combustion. Coal is not completely combusted in a burner; instead, it is gasified in a gasifier to turn carbon mainly into CO. Then, a shift reaction involving H_2O takes place, where H_2O and CO react to become H_2 and CO_2. Products from this pre-combustion step finally go into carbonator and then into calciner.

Both post-combustion capture and pre-combustion capture are modeled in the thesis using ASPEN PLUS.

Only thermal energy analysis is performed; thus the turbines and generators in the power plant are not included. Since heat does not transform into other forms of energy (i.e. the mechanical energy or electrical energy), the term 'heat' is used in most places in the thesis instead of the term 'energy.'

3.1 Model Setup for Post-combustion Capture

Since we are interested in the overall heat production from a power plant without and with Calcium looping, all inlet materials are set at room temperature and the inlet coal properties are set as received rather than using those of dry coal.

We begin by defining all the components. These include both conventional and nonconventional components. Pure materials are designated as 'conventional', including all possible simple substances and chemical compounds for elements C, N, O, H, S, and Cl which might be produced during the chemical reactions including the important compounds CaO and $CaCO_3$.These properties can be obtained from ASPEN PLUS data bank. Mixtures are designated as 'nonconventional', including coal and ash. Table 3.1 provides a list of all the components used in the modeling.

Table 3.1: Components predefined in ASPEN PLUS

Component name	Chemical formula	Type
Carbon-graphite	C	Solid
Carbon-monoxide	CO	Conventional
Carbon-dioxide	CO_2	Conventional
Carbonyl-sulfide	COS	Conventional
Methane	CH_4	Conventional
Ethylene	C_2H_4	Conventional
Ethane	C_2H_6	Conventional
Hydrogen	H_2	Conventional
Water	H_2O	Conventional
Hydrogen-chloride	HCl	Conventional
Hydrogen-sulfide	H_2S	Conventional
Calcium-oxide	CaO	Conventional
Calcium-carbonate-calcite	$CaCO_3$	Conventional
Calcium-sulfide	CaS	Conventional
Coal	-	Nonconventional
Ash	-	Nonconventional
Oxygen	O_2	Conventional
Nitrogen	N_2	Conventional

Nitric-oxide	NO	Conventional
Nitrogen-dioxide	NO_2	Conventional
Nitrous-oxide	N_2O	Conventional
Ammonia	NH_3	Conventional
Sulfur	S	Conventional
Sulfur-dioxide	SO_2	Conventional
Sulfur-trioxide	SO_3	Conventional
Chlorine	Cl_2	Conventional

3.1.1 Combustor Setup

Illinois #6 coal is used in the simulation; it is the same coal that was used in the simulation by Sivalingam (2013). The 50 kg/s flow rate of coal was used by Sivalingam (2013) which is a large number. Therefore, a 5 kg/s of coal inflow is also calculated as another case. In ASPEN PLUS, the coal is defined as a nonconventional component; its specific attributes are set in the flow sheet when editing the material stream 'coal'. Open component attribute drop down list in ASPEN PLUS, enter the proximate analysis, ultimate analysis (Sivalingam 2013) and sulfur analysis data to define the coal. Specific values for coal properties are listed in Tables 3.2, 3.3 and 3.4.

Table 3.2: Proximate analysis of Illinois #6 coal (Sivalingam 2013)

Constituents	Weight percentage (%)
Moisture	11.12
Fixed carbon	44.19
Volatiles	34.99
Ash	9.7

Table 3.3: Ultimate analysis of Illinois #6 coal (Sivalingam 2013)

Constituents	Weight percentage after drying (%)	Weight percentage as received (%)
Moisture	0	11.12
Ash	10.91	9.7
Carbon	71.72	63.75
Hydrogen	5.06	4.5
Nitrogen	1.41	1.25
Chlorine	0.33	0.29
Sulfur	2.82	2.51
Oxygen	7.75	6.88

Table 3.4: Sulfur analysis of Illinois #6 coal

Constituents	Weight percentage (%)
Pyritic	1
Sulfate	1
Organic	0.82

The percentages of sulfur analysis should add up to be equal to the weight percentage of sulfur in the ultimate analysis of dried coal. Differences in sulfur analysis won't affect the burning heat of the coal. Since the data for sulfur analysis is not easily available, a reasonably good guess of the numbers in Table 3.4 was made.

In ASPEN PLUS modeling, coal cannot be directly burned as a nonconventional material. Therfore, the 'RYIELD' reactor is employed to transform the coal into various conventional materials; this process is called the 'decomposition'. Temperature is set at 1198.15 K (925 °C), and the pressure is set at 1 bar. This reactor allows the user to define the products for a chemical reaction. Whatever products may be result from decomposition, as long as various elements are in balance, it won't make any difference on the total heat from the combined decomposition and burning. Thus the products of decomposition are set as the simplest components: Ash, H_2O, C, H_2, N_2, Cl_2, S, and O_2. Mass percentages for the component yields are obtained based on the ultimate analysis of coal (using weight percentage as received) in Table 3.3. In the reactor block of decomposition, the nonconventional material 'ash' is defined (Table 3.5) to have 100% of 'ash'; 'ash' is a predefined material in ASPEN PLUS used for defining the coal.

Table 3.5: Ultimate analysis of ash

Constituents	Weight percentage (%)
Ash	100
Carbon	0

After decomposition, material stream goes into a burner, which is the 'RGIBBS' reactor in ASPEN PLUS. RGIBBS is a reactor that can automatically calculate the products when reaching equilibrium under certain pressure and temperature. We exercise the option that 'calculates the phase equilibrium and chemical equilibrium'. Pressure is set at 1 bar, temperature is set at 1673.15 K (1400 °C). Air is another material stream that enters the burner. Air amount should be set such that all the carbon turns into carbon dioxide, but it should not be more – more air will lower the heat output. The calculation for the proper amount of air is discussed in the sessions on data analysis.

After burning, materials are taken to a separator ' SSPLIT' to separate ash from other conventional materials. Ash is then thrown away, but before that, a heat exchanger ('Heater') is inserted in the stream to lower the temperature to 150 °C. The addition of a heat exchanger and its simplifications are discussed in section 3.1.4.

At this stage, the coal is considered completely combusted, and the produced flue gas is cooled to 150 °C, which then undergoes the Calcium looping. Heat absorbed from cooling the flue gas is attributed as the heat of combustion.

3.1.2 Carbonator Setup

Carbonator refers to the reactor where CaO and CO_2 react to form $CaCO_3$. Calciner refers to a reactor where $CaCO_3$ breaks down to form CaO and CO_2.

ASPEN PLUS cannot simulate a looping process, therefore a serial process is employed, to model the Calcium looping. In the serial process, a carbonator is used to absorb certain amount of CO_2 and then a calciner is used to break down all the $CaCO_3$ produced in the carbonator.
In ASPEN PLUS, 'RSTOIC' block is used as carbonator. Temperature is set at 650 °C and pressure is set at 1 bar. RSTOIC is reactor in which the user can define specific reaction that happen. Reaction takes place in a stoichiometric manner, with constraint on conversion fraction of one reactant. Chemical reaction equation is expressed by Equation 3.1.

$$CaO + CO_2 = CaCO_3 \quad (3.1)$$

In real situations, CaO and CO_2 do not react completely with each other. The amount of CaO that can actually react is constrained by the surface area of CaO particles. Furthermore the mixing between CO_2 and CaO is affected by how the fluidization develops in the reactor. Finally, the speed of reaction is restricted by the rate of chemical reaction. Considering these three aspects, it turns out that given a certain flow rate of CO_2, not all of these effects can be captured in the carbonator for any given amount of CaO.

In 'RSTOICH' reactor in ASPEN PLUS, the only way to manipulate a reaction other than defining it by an equation is to define the extent of the reaction. To define the extent of reaction, the value of the conversion fraction for one of the reactant can be specified. Thus the conversion fraction of CaO is predefined in 'RSTOICH' reactor. It is defined using information from experimental data.

Experimental results on CO_2 capture efficiency, CO_2 flow rate and CaO flow rate given by Abanades et al (2005) are shown in Figure 3.1.

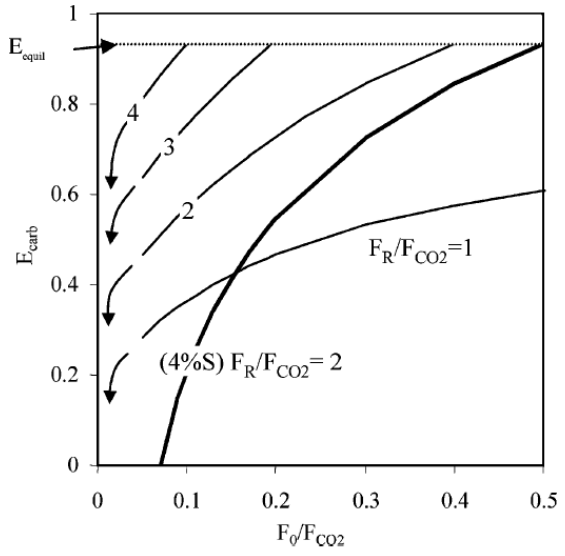

Figure 3.1: CO2 capture efficiency under different flow rates of CaO and CO2 (Abanades et al, 2005)

Table 3.6: CO2 capture efficiency under different flow rates of CaO and CO2 (Sivalingam 2013)

F_o/F_{CO_2}	E_{CO_2}		
	$F_R/F_{CO_2} = 3$	$F_R/F_{CO_2} = 4$	$F_R/F_{CO_2} = 5$
0.05	0.63	0.81	0.99
0.1	0.76	0.95	0.99

In Figure 3.1 and Table 3.6, E_{CO_2} refers to CO_2 capture efficiency, F_{CO_2} refers to the mole flow rate of CO_2, F_R refers to the flow rate of recycled CaO in the bed and F_o refers to the make-up flow of CaO.

Figure 3.1 has been translated into a table format by Sivalingam (2013). The part of that table used in this thesis is shown in Table 3.5.

It is not possible to model the make-up flow in ASPEN Plus, therefore one value of F_o/F_{CO_2} is chosen to obtain one set of data for calculation. $F_o/F_{CO_2} = 0.1$ is chosen with three values of F_R/F_{CO_2} such that the CO_2 capture efficiency is in the range of 50% to 100%.

For a certain flow ratio and CO_2 capture efficiency, there is certain associated CaO conversion fraction. Since CO_2 capture efficiency cannot be directly controlled, multiple cases are run in ASPEN Plus for a certain CaO conversion fraction in order to obtain a correct CO_2 capture efficiency. As shown in Table 3.7, specified a CaO conversion fraction will correspond to a range of CO_2 capture efficiency. As shown in Figure 3.2, small symbols (dots and triangles) refer to the trial cases conducted in ASPEN Plus; these will be called the results calculated from extrapolated data in future discussions. Large symbols refer to cases whose results fit the experimental data; these cases will be called results obtained from experimental data in the future discussions.

Table 3.7: Range of CO2 capture efficiency for each CaO conversion fraction

F_R/F_{CO_2}	CaO conversion fraction	E_{CO_2} range
3	0.33	0.66 ~ 0.86
4	0.25	0.86 ~ 0.97
5	0.2	0.97 ~ 0.99

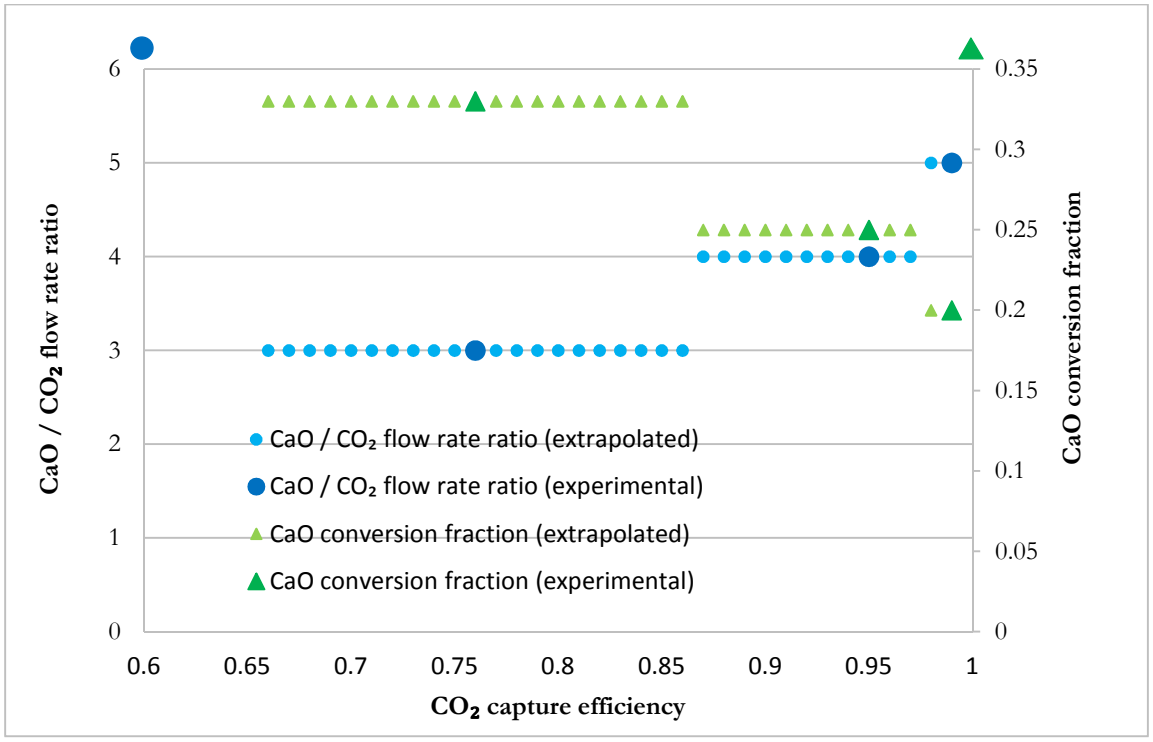

Figure 3.2: Corresponding range of CO2 capture efficiency for various CaO conversion fraction

Down-stream of carbonator, a mixture of $CaCO_3$ and what is left in the flue gas is obtained. The mixture goes through a heat exchanger to cool down to 150 °C and returns the heat released during the cooling-down process back to the carbonator. This is a way to account for the heat of carbonation and calcination separately.

The stream then goes through a separator ('Sep block') to separate the gases from the solid. The gases are relatively CO_2-lean compared to the original flue gas. Solid is pure $CaCO_3$, if the inlet CaO low rate does not exceed a certain amount. CaO inlet flow rate is a variable that can be used to control the CO_2 capture efficiency and the total heat output.

3.1.3 Calciner Setup

Similar to Carbonator, 'RSTOIC' reactor block is employed for calciner in ASPEN Plus.The reaction is as follows:

$$CaCO_3 = CaO + CO_2 \tag{3.2}$$

The temperature in this block is 900 °C and the pressure is 1 bar.

Unlike carbonation, calcination reaction is a fully completed reaction, thus all $CaCO_3$ is decomposed. Therefore the conversion fraction of $CaCO_3$ is set at 1.

Post-stream of calciner again goes through a heat exchanger then a separator like before. Heat absorbed from this heat exchanger is added to the heat of calciner.

3.1.4 Summary for Post-combustion Model Setup

The reactor blocks used in ASPEN Plus along with their functions and reaction formulas are listed in Table 3.8.

Table 3.8: Process models used for post-combustion setup in ASPEN Plus

Name	Reactor Model	Function	Reaction formula
DECOMP	RYIELD	Turn non-conventional into conventional	Coal → char + simple substances
BURN	RGIBBS	Coal burns with air	Char + simple substances + O_2 → CO_2 + H_2O
CARBONAT	RSTOIC	Carbonation	$CaO + CO_2 \rightarrow CaCO_3$
CALCINER	RSTOIC	Calcination	$CaCO_3 \rightarrow CaO + CO_2$
SEP-ASH	SSPLIT	Flue gas and ash separation	-
SEP-CAR	SEP	Flue gas (CO_2 lean) and Ca solids separation	-
SEP-CAL	SEP	CO_2 and Ca solids separation	-
COOL-A	HEATER	Ash cooler	-
COOL-B	HEATER	Flue gas cooler	-
COOL-C	HEATER	Cooler downstream of carbonator	-
COOL-D	HEATER	Cooler downstream of calciner	-

The temperatures and pressures for various reactor in Table 3.8 are summarized in Table 3.9.

Table 3.9: Temperature and pressure specification for each block of Table 3.8

Block name	Temperature (K)	Pressure (bar)
Decomposition	1198.15	1
Burner	1673.15	1
Carbonator	923.15	1
Calciner	1173.15	1
All separators	-	-
All heaters	423.15	1

The explanation for the necessity of adding heaters is as follows. To maintain a predefined fixed temperature for each reactor, the heat produced or absorbed in a reaction will have to transmit in two ways. One way is to change the amount of heat in each reactor; the other way is to change the temperature of the outlet flow. These two ways need to be simultaneously considered in the overall heat balance. Thus, to keep track of the total heat produced or absorbed by a reaction, these two parts of heat need to be accounted together. For example, if the outlet stream of a reactor is too hot, it indicates that some heat produced by this reaction is transmitted to by this stream. Via a heat exchanger (which is a 'Heater' block), one can lower the temperature of this outlet steam, and return that amount of heat back to the reactor. The combination of reactor and heater to accomplish this process is shown in Figure 3.3.

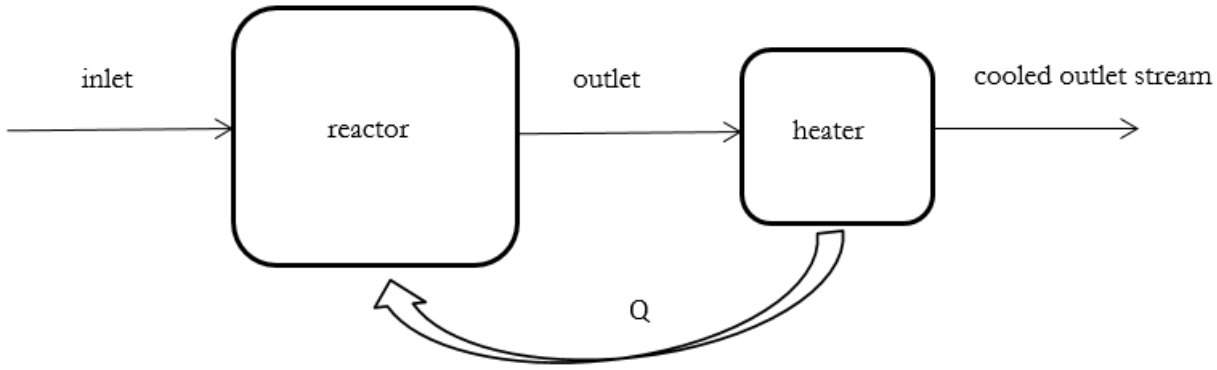

Figure 3.3: The scheme of adding a heater down stream of each reactor

All heaters need to be set at the same temperature. This temperature cannot be too low, since there is the lowest limit for the power plant flue gas temperature, which is chosen to be 150 ºC (423.15 K); it is within the range given by Feron (2008).

For the heat stream, we add up the heat from decomposer, burner, heat exchanger for ash and heat exchanger for flue gas together to be the heat of coal burning without Calcium looping. Then the rest of the heat—heat of carbonator, post-carbonator heat exchanger, calciner and post-calciner heat exchanger together becomes the heat of Calcium looping. These two values of heat and the CO_2 fraction in the final outlet flow are indicative of the performance of Calcium looping with post-combustion capture. The heat values of carbonation and are also of interest in the evaluation of the performance of Calcium looping with post combustion capture.

The flow sheet setup in ASPEN Plus is shown in Figure 3.4.

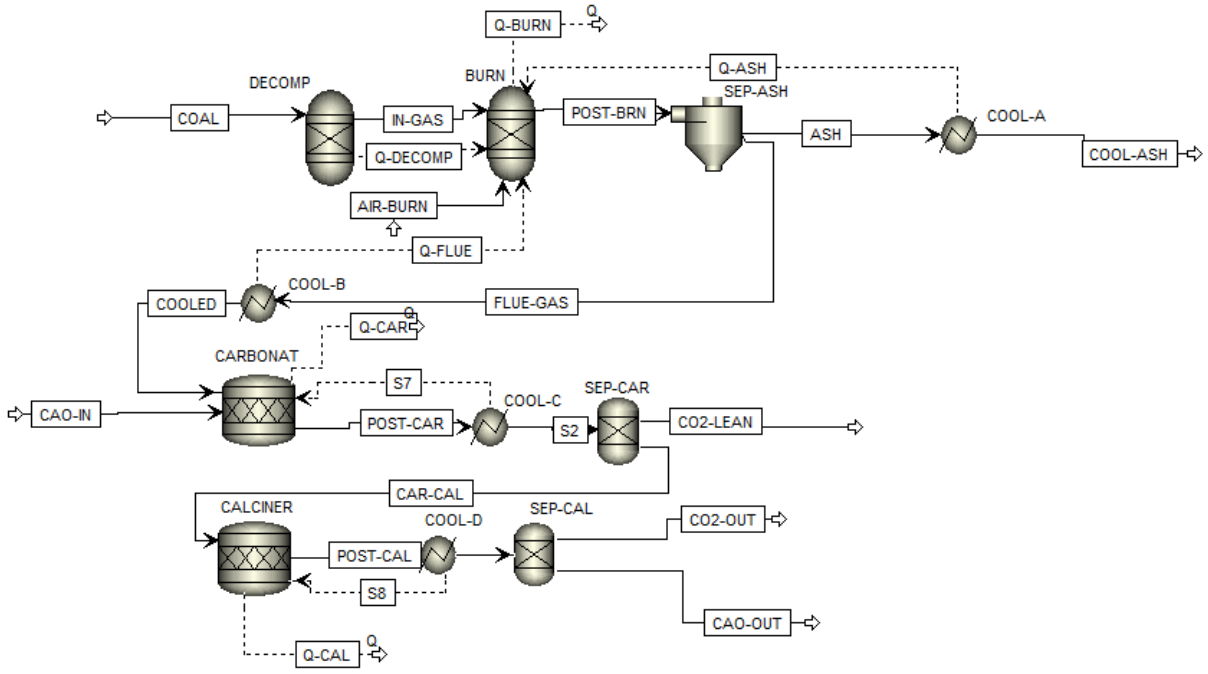

Figure 3.4: The Calcium looping flow sheet in ASPEN Plus for post-combustion capture

3.2 Data Analysis for Post-combustion Capture

3.2.1 Calculation of the Required Amount of Air

It is not possible to input 'air' in ASPEN Plus, therefore when changing the air flow rate as a variable, one needs to change O_2 and N_2 separately by assuming that air only consists of O_2 and N_2, since other components of air will have almost no effect on the results.

We employ 'optimization' under 'Model Analysis Tools' to find proper values for O_2 and N_2 flow rates. Optimization setup and results are shown in Table 3.10 and Table 3.11. $F_{CO}, F_{CO_2}, F_{O_2}$ and F_{N_2} refer to the mole flow rate of indicated gas component (CO and CO_2 for downstream of the burner, O_2 and N_2 for upstream of the burner).

Table 3.10: Optimization variables setup and results

	O_2	N_2
Manipulation range (kmol/s)	3 ~ 5	12 ~ 16
Maximum step size (kmol/s)	0.5	0.5
Optimized result (kmol/s)	4.2	15.76

Table 3.11: Constraints and convergence results for optimization of amount of air

Convergence criteria	Tolerance	Result
$F_{CO} = 0.001$ kmol/s	0.001 kmol/s	0.00059 kmol/s
$F_{O_2}/F_{N_2} = 0.2658$	0.01	0.2664
Maximize F_{CO_2}	-	2.653 kmol/s

The basic idea behind the optimization is to change O_2 and N_2 flow rates separately within a small range, in order to get the maximum CO_2 flow out of the burner. Constraints for this process cover the flow rate of CO out of burner, and flow rate ratio between O_2 and N_2. This will assure that nearly all the coal burned is CO_2, with smallest amount of O_2 and N_2, while the ratio between O_2 and N_2 is the same as that in the air.

After optimization, O_2 and N_2 flow rates are 4.2 kmol/s and 15.76 kmol/s corresponding to 50 kg/s of coal. O_2 and N_2 add up to nearly 20 kmol/s of air flow, therefore 20 kmol/s of air flow is used at the burner.

For scaled higher coal flow rate cases, O_2 and N_2 flow rates are changed proportionally.

3.2.2 Carbonation and Calcination Analysis

The objective of Calcium looping is to reduce the amount of CO_2 released into the atmosphere. Therefore the CO_2 capture efficiency is the most important quantity. Hence the CO_2 capture efficiency is employed as a variable on the x axis, and all other quantities of interest are plotted on on the y axis to examine how the CO_2 capture efficiency affects changes in other quantities.

Since there is no other energy loss that needs to be considered, the summation of heat gain and loss in carbonation and calcination would be equal to the heat penalty interested in Calcium looping.

For each CaO conversion fraction, there is a corresponding CO_2 capture efficiency from the experimental data. Once the CaO conversion fraction is predefined, by changing the CaO inflow to the carbonator, one can manipulate the CO_2 capture efficiency so as to be equal to the experimental result. With change in CaO inflow, the heat duty of the carbonator and calciner will change. Therefore, for each pair of experimental data, one can calculate one data point of heat duty for carbonator and calciner.

There is a way to obtain more data points by extrapolation based on the experimental data. For each CaO conversion fraction, we can calculate a range of CO_2 capture efficiencies, instead of just one.

Both the results from original data (non-extrapolated) and extrapolated data are shown in Figure 3.5.

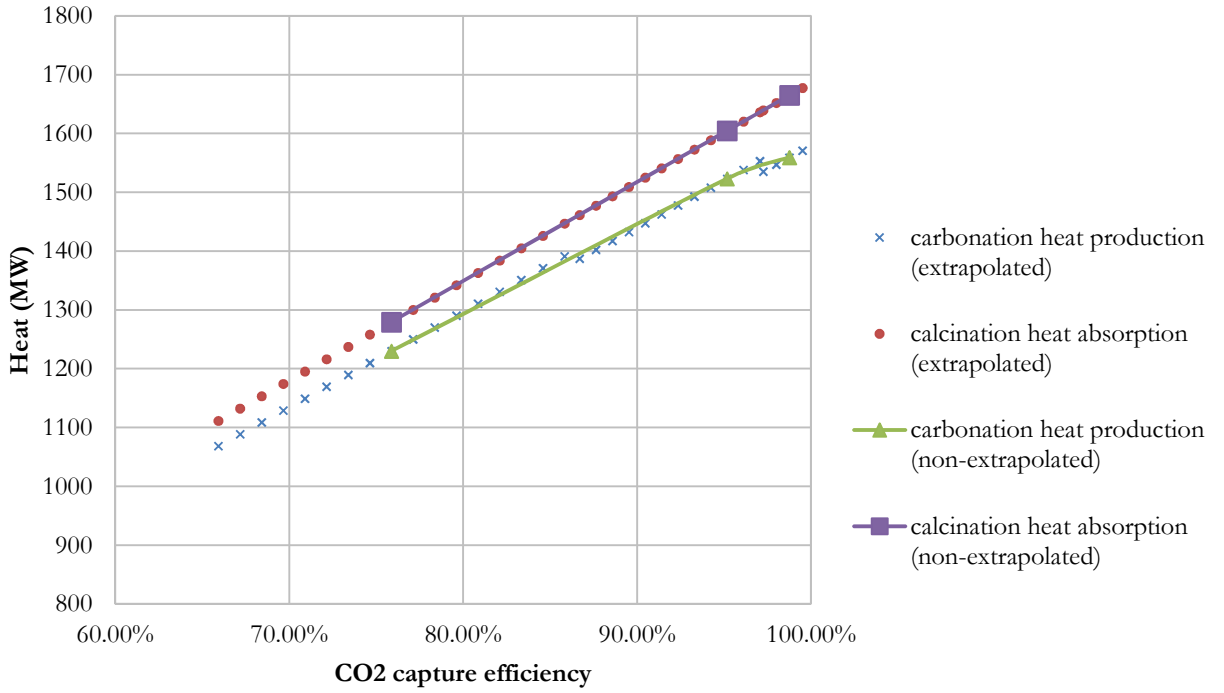

Figure 3.5: The heat gain and loss in carbonator and calciner (calculated from original experimental data and extrapolated experimental data)

Since calcination is an endothermic reaction (a reaction absorbing heat), the heat duty calculated in ASPEN Plus will be a negative number. In order to compare the two reactions, we use the absolute value of carbonation heat duty and express it as the heat absorption of calcination.

There are two ways of calculating and processing the data. One way is to extrapolate between experimental data points to obtain a series of input data values for the ASPEN Plus solver and then performing the calculations to get a series of results. The second way is to use only three available experimental data points to calculate only three results and then drawing a smooth curve through these three results; we call this the non-extrapolation method.

The reasons for calculating the data in two ways decided above can be summarized as follows. First reason is that it is not possible to get accurate results in the region between the two experimental data points. Therefore extrapolation of data between the experimental data points may be necessary. Second reason is that there may be some regions where the extrapolation method may give more accurate results than simply using the experimental data points and fitting a smooth curve.

It can be observed from Figure 3.5 that the results of calcination form almost a linear line, and the two methods described above coincide with each other. This linearity is expected, since the calculation is based on a stoichiometric relation, which implies that, for any incoming rate of one reactant, there is a proportional incoming rate of the other reactant to react with it, resulting in the heat produced also proportional to the incoming rate of reactant. And as shown in Figure 3.5, the CaO conversion fraction does not affect this linear relation. This is because the calciner has the same temperature for both inlet and outlet flow (both are at 150 ºC). When there is an excess amount of CaO into the carbonator, the unreacted CaO will pass through the carbonator and enters the calciner; this unreacted part of CaO has no effect on the reaction within the calciner. Thus the heat duty of calciner remains unchanged by the excess amount of CaO.

For the carbonator, the data points from the extrapolation method seem to form three sections, and each section is a straight line. The linearity of these sections can be explained the same way as for the calciner. However in this case, the CaO conversion fraction has some effect. Each straight line section (corresponding to a range of extrapolated data) has a vertically negative displacement compared to the previous section. And the slope of these lines is less steep than for the case of calciner. From the modeling point of view, the only difference between these two reactors, beside the chemical reaction, is the inlet stream temperature. The carbonator has a 25 ºC inlet stream, compared to the calciner's 150 ºC, while both the carbonator and the calciner have the 150 ºC outlet stream. Thus some heat is consumed simply for heating up the inlet stream to the temperature of the outlet. This is the main reason for different behavior of calciner and carbonator as described above. Furthermore, since the inlet and outlet stream of a reactor have different composition of species with different heat capacity is continuously changing; it leads to difficulty in calculating the heat absorbed due to temperature change.

Finally comparing the extrapolation and non-extrapolation method, there does not appear to be much difference. It can observed that the curve for carbonator has a gradually decreasing slope.

3.2.3 Energy Penalty Analysis

For a 50 kg/s of inlet coal flow, the heat of combustion is calculated to be 1168 MW. This compares well to the total heat of the power plant when including Calcium looping, which ranges from 1060 to 1130 MW. This is shown in Figure 3.6.

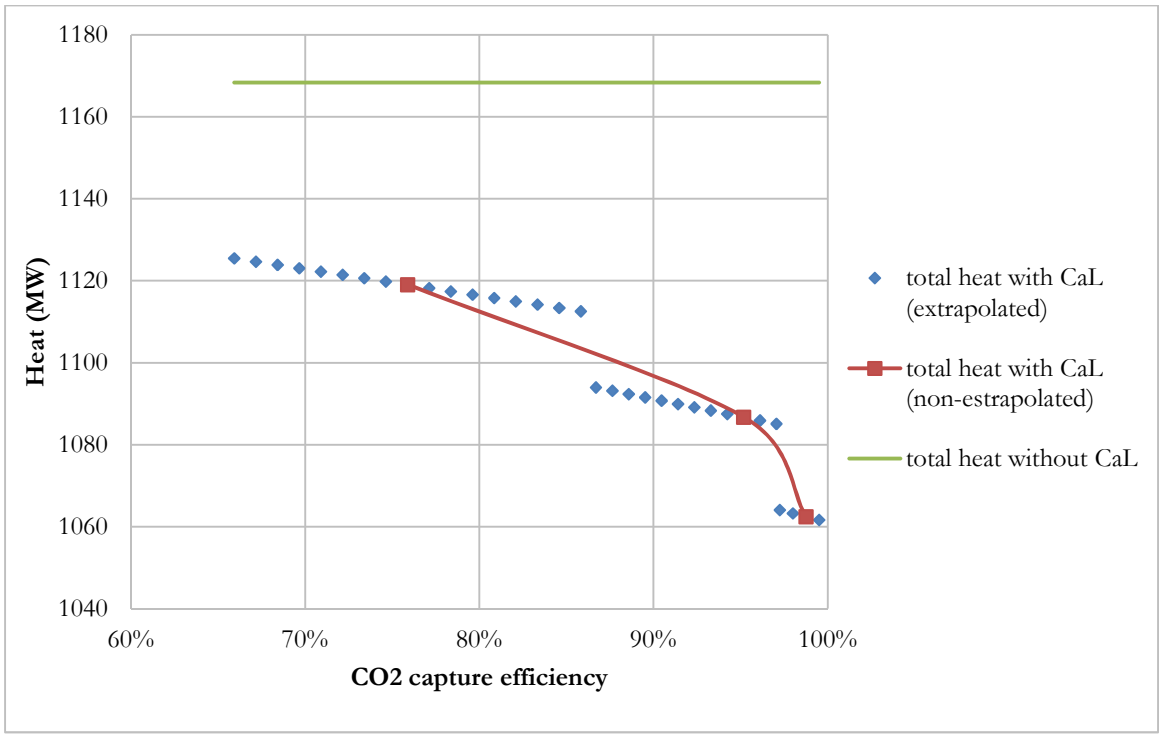

Figure 3.6: Total energy (heat) output for post-combustion setup, with and without CaL

Energy penalty for Calcium looping refers to the fraction of energy produced by a power station that must be dedicated to CaL process in order to capture CO_2.

To obtain the energy penalty, we use the following equations:

$$Q_{total} = Q_{coal} - |Q_{looping}| \quad (3.3)$$

$$p = (|Q_{looping}| / Q_{total}) \times 100\% \quad (3.4)$$

p: energy penalty for adding Calcium looping to a power plant

Q_{total}: total heat produced by a power plant

Q_{coal}: heat produced by a power plant without Calcium looping

$Q_{looping}$: heat for Calcium looping

Figure 3.7 shows the energy penalty calculated from equations (3.3) and (3.4). From this figure, energy penalty ranges from 3.5% to 9%, with corresponding CO_2 capture efficiency ranging from 65% to 99%. For different power plants, Cormos and Petrescu (2014) have calculated the CO_2 capture efficiency ranging from 92% to 93%, and energy penalty ranging from 5% to 10%. Many articles in the literature also shows that the energy penalty for high-efficiency post-combustion carbon capture greater than 90% is roughly near 10%, which is close to the present result of 9% in this thesis.

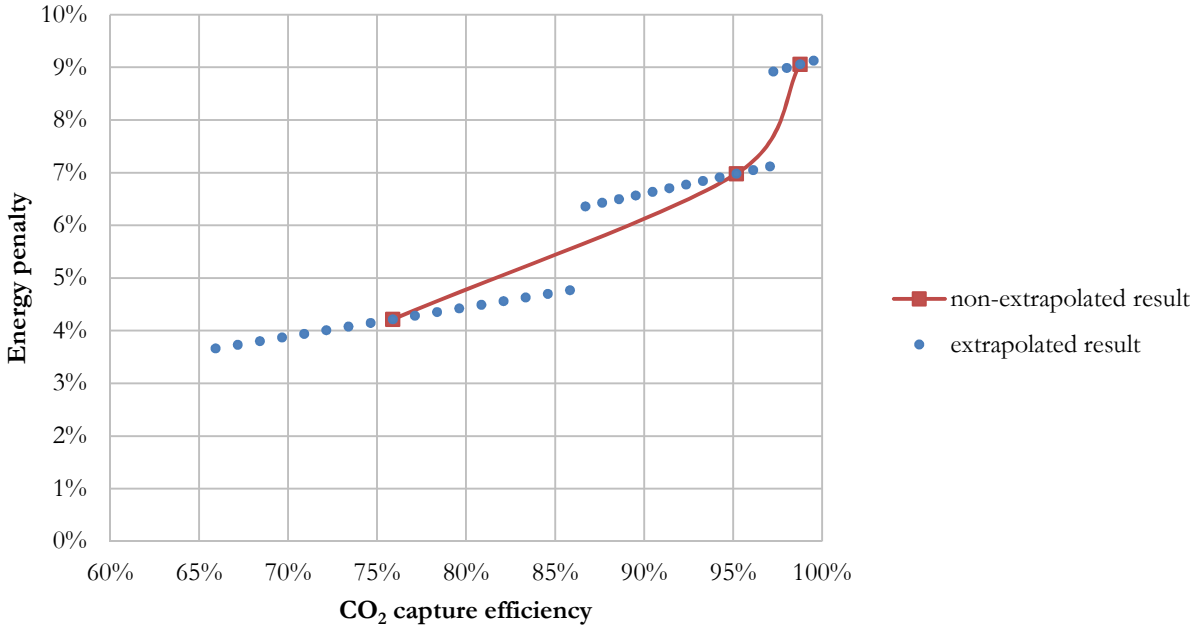

Figure 3.7: Energy penalty vs. CO2 capture efficiency in post-combustion carbon capture

Figure 3.7 has shape similar to that for total energy (heat) as shown in Figure 3.6 since the results in Figure 3.7 are calculated from Figure 3.6. From Figure 3.6, it can be observed that the result obtained calculated from the extrapolated data form three sections of straight lines. The fitted curve (in red) connecting the three points from the experimental data also shows a gradually increasing

slope. The straight lines in Figure 3.7 are similar to these obtained in the previous analysis of carbonator and calciner.

Since Figure 3.7 has obvious jumps among the three straight line sections of results obtained from extrapolation of experimental data, and these extrapolated results denoted by blue dots are not close to the smooth red curve connecting the results obtained from the original experimental data, comparison between the two approached is not expected to be close. At first glance, the red curve looks more reasonable and the blue dots seem not to be an accurate representative because of jump between the three straight lines. However the blue dots results are actually calculated by extrapolation of the three experimental points. The red curve simply represents a curve-fit connecting the three points. For more accurate calculations to determine how the energy penalty varies with the CO_2 capture efficiency, the combination of these two methods may be desirable. Since the blue dots show linear relation in certain range, it could be used to extrapolate between the blue dots for a given straight line. However, in the regions where there is jump between the two straight lines, it may be desirable to create an appropriate smooth curve.

A summary of simplifications made in obtaining the above results is given below. In the results presented above only the heat output of CaL is assessed. In a whole plant, heat generated from coal combustion will heat up the steam to drive a steam turbine connected to an electric generator to generate electricity. Thus, the difference of temperature matters in the whole power plant, even with some heat sources having the same amount of thermal energy; difference in temperature can lead to different amount of electricity generated due to these sources. In many papers, the energy penalty is calculated based on the electric power generated by the whole power plant. In this thesis, the energy penalty is calculated based only on the heat of coal combustion, therefore the effect of high temperature is not reflected in the present model. It is assumed that all heat sources can contribute to energy until they reach a temperature as low as 150 ºC. Furthermore, when considering the whole plant, transportation of the solid calcium will cost extra energy.

In summary, we have considered a very simplified model of Calcium looping, which only takes into account the heat of chemical reaction in a stoichiometric fashion. Thus the energy penalty calculated

from this simplified model should be considered as a lower bound for any investigation on Calcium looping.

3.3 Model Setup for Pre-combustion Capture

3.3.1 Gasifier Setup

Here, H_2O is used instead of O_2 for gasification. In most cases, coal gasification uses O_2 from an Air Separation Unit to burn the coal to get CO and some H_2, while avoiding production of CO_2 and H_2O. From an energy point of view, as long as the coal is burnt to its final products, the heat produced in the gasification process will remain the same. Thus to simplify gasification H_2O is used in this work. Heat for gasification is provided from sources other than by burning of carbon; however it makes no difference to the final results. The only difference is that there is no air separation unit in the present model. The calculation thus accounts for less amount of energy loss, since air separation unit consumes a significant amount of energy.

Using again the 'RGIBBS' block as a burner and the same flow sheet model in ASPEN Plus as for the post-combustion capture, the gasifier differs in the pre-combustion capture in the sense that it does not completely burn the coal. Instead of reacting with air, the coal reacts with the steam. The reaction is as follows:

$$H_2O + C = H_2 + CO \tag{3.5}$$

We choose the 'calculate phase equilibrium and chemical equilibrium' option in ASPEN Plus, and set the pressure at 1 bar and temperature at 1673.15 K.

3.3.2 Carbonator and Calciner

Carbonator now divides into two parts: carbonator 1 and carbonator 2.

Carbonator 1 is where the shift reaction takes place. The stream of syngas contains H_2 and CO. The purpose of shift reaction is to turn CO into CO_2 with steam, while H_2 can be produced. The reaction is:

$$H_2O + CO = H_2 + CO_2 \quad (3.6)$$

Carbonator 2 is the same carbonator as in post-combustion capture. Stream going through this carbonator will have the CO_2 captured. Reaction is same as in equation (3.1). Calciner has the same setup as in post-combustion capture.

3.3.3 Hydrogen Burner

As mentioned above, H_2 is produced in the pre-combustion capture. To evaluate the amount of energy produced, entire H_2 is simply burnt. The burnt H_2 is then used to heat up steam.

Thus in the pre-combustion set up, an additional reactor is used to burn the H_2 produced. The inlet air temperature for this hydrogen burner is set at 150 ºC, which is the same as final outlet temperature. This is done in order to maintain sufficient air amount for different flow rates of H_2. In some cases the air amount may be in excess for low rate of H_2. In this situation, if the inlet air is at 25 ºC and is in excess for a particular case, some energy will be wasted to heat up the extra air to 150 ºC. By setting the inlet air temperature at 150 ºC, the influence of air amount is eliminated.

3.3.4 Summary of Pre-combustion Model Setup

Various reactor blocks used in ASPEN Plus and their specifications for pre-combustion capture are listed in Table 3.12.

Table 3.12: Process models used for pre-combustion setup in ASPEN Plus

Name	Model	Function	Reaction formula
DECOMP	RYIELD	Turn non-conventional into conventional	Coal → char + simple substances
GASIFIER	RGIBBS	Coal gasifies with steam	Char + simple substances + H_2O → CO + H_2 + volatile matter
CARBONAT1	RSTOIC	Shift CO to be CO_2 and produce H_2	CO + volatile matter + H_2O → CO_2 + H_2
CARBONAT2	RSTOIC	Carbonation	$CaO + CO_2 \rightarrow CaCO_3$
H2-BURN	RSTOIC	Combustion of H_2	$H_2 + O_2 \rightarrow H_2O$
CALCINER	RSTOIC	Calcination	$CaCO_3 \rightarrow CaO + CO_2$
SEP-ASH	SSPLIT	Flue gas and ash separation	-
SEP-CAR	SEP	Flue gas (CO_2 lean) and Ca solids separation	-
SEP-CAL	SEP	CO_2 and Ca solids separation	-
COOL-A	HEATER	Ash cooler	-
COOL-B	HEATER	Flue gas cooler	-
COOL-C	HEATER	Carbonator downstream cooler	-
COOL-D	HEATER	Downstream cooler for H_2 burner	-
COOL-E	HEATER	Calciner downstream cooler	-

Temperature and pressure settings for all blocks in Table 3.12 are shown in Table 3.13. The flow sheet setup in ASPEN Plus is shown in Figure 3.8.

Table 3.13: Temperature and pressure specification for each block (pre-combustion) in ASPEN Plus

Block name	Temperature (K)	Pressure (bar)
Decomposition	1198.15	1
Gasifier	1673.15	1
Carbonator 1	923.15	1
Carbonator 2	923.15	1
H_2 burner	1673.15	1
Calciner	1173.15	1
All separators	-	-
All heaters	423.15	1

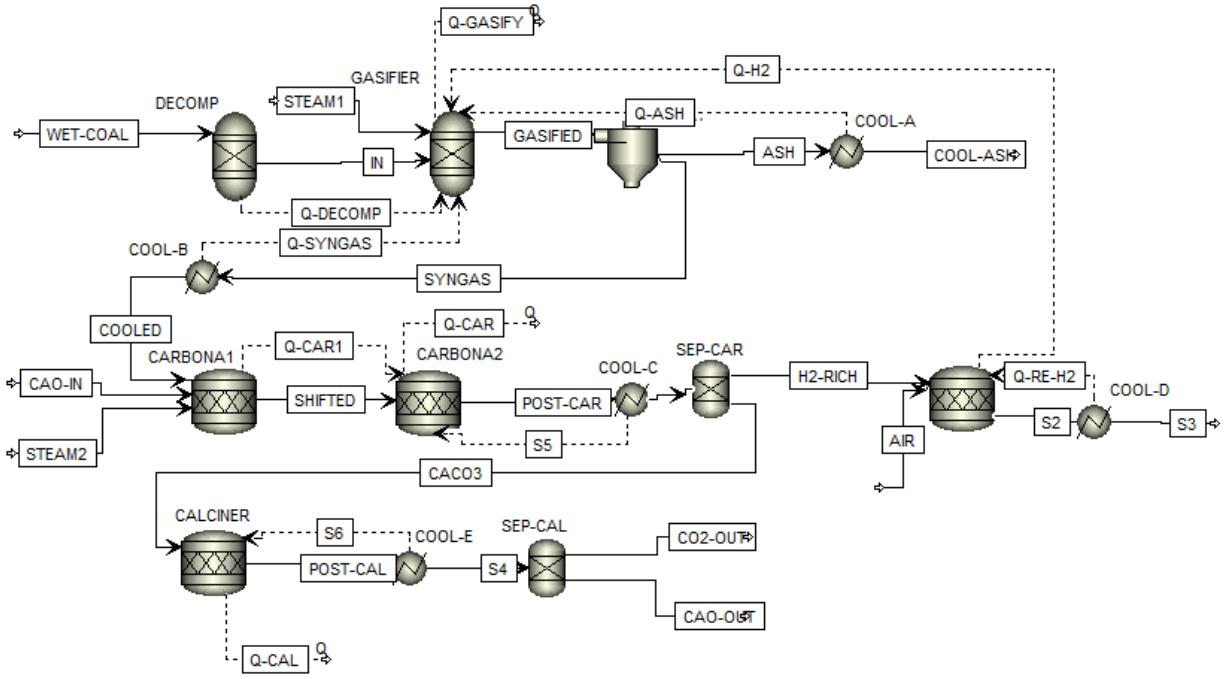

Figure 3.8: The Calcium looping flow sheet in ASPEN Plus for pre-combustion capture

3.4 Data Analysis of Pre-combustion Capture

3.4.1 Calculation of the H_2O Flow Rate Needed for Gasifier

The reaction between coal and steam is broken into two parts, first turning all C into CO and then turning all CO into CO_2. The first part takes place in the gasifier. The goal for this part is to have maximum CO output, which is the needed for H_2 production in the second reaction.

A 'sensitivity analysis' is employed to achieve this goal. As shown in Figure 3.9, steam flow rate is varied from 0 to 3 kmol/s, and C, CO and CO_2 flow rates are monitored in the successive stream.

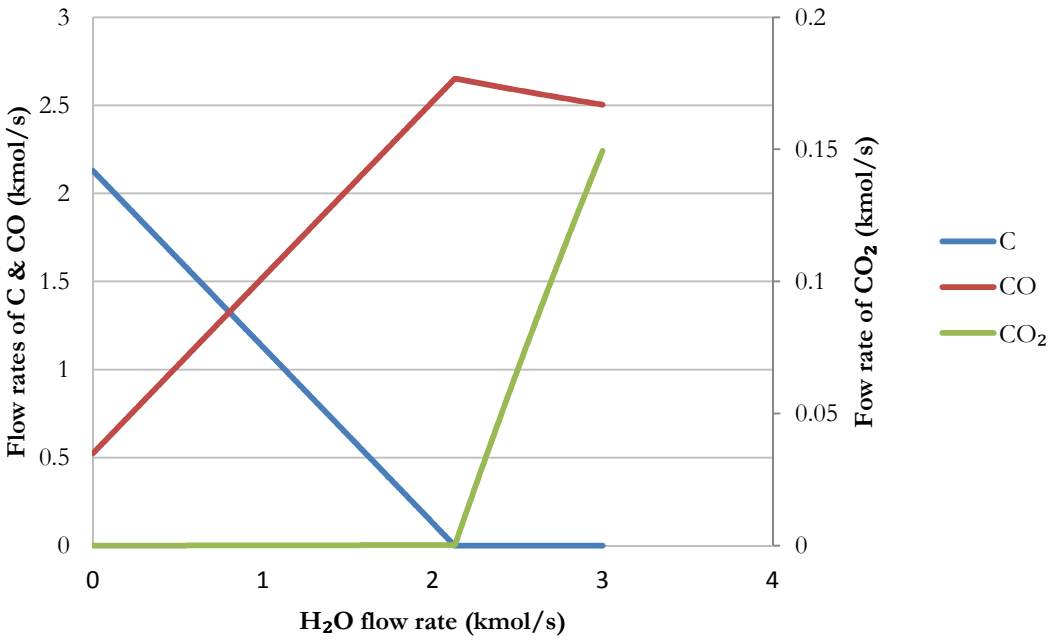

Figure 3.9: Variation in gasifier outflow components with H_2O inflow rate

It can be observed from Figure 3.9 that at 2.1 mole flow rate of H_2O, all carbon C is burnt and CO_2 starts to form, and CO begins to decrease.

3.4.2 Calculation of the H_2O Flow Rate Needed for Carbonator

Carbonator 1 converts all CO into CO_2 and produces H_2. Thus the steam flow rate should be such that it results in all CO to be completely converted.

Figure 3.10 shows how the flow rates of CO, CO_2 and H_2 are influenced by the flow rate of H_2O.

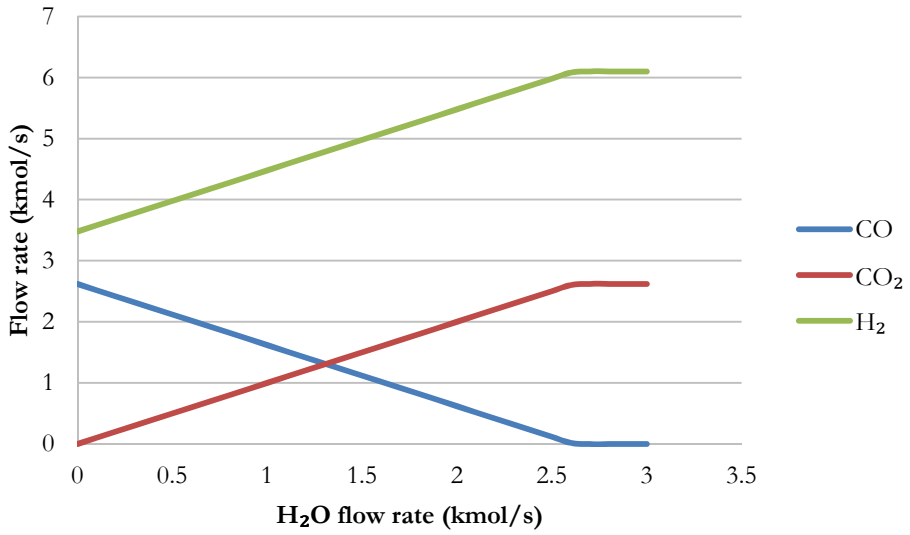

Figure 3.10: Carbonator 1 outflow component vs. inflow H2O

From Figure 3.10 it can be seen that the steam flow should be 2.7 kmol/s when all CO is consumed and H_2 and CO_2 flow rates acquire the highest possible value.

3.4.3 Energy Penalty Analysis

Without Calcium looping, for pre-combustion capture, the total heat of coal gasification and H_2 combustion combined is 1132 MW. The total heat with CaL ranges from 980 to 1060 MW. This is shown in Figure 3.11.

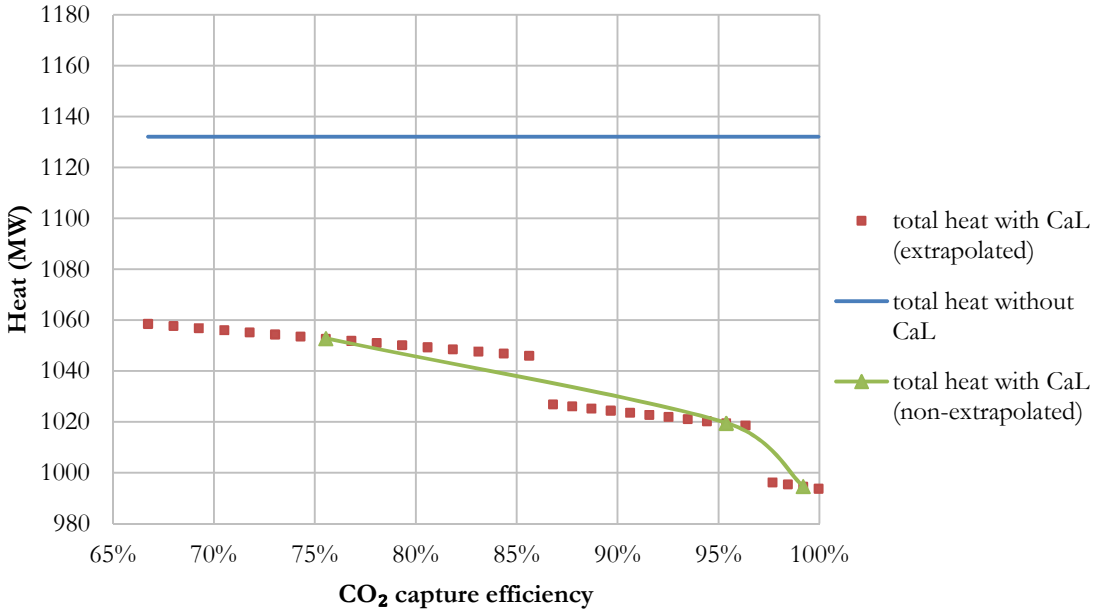

Figure 3.11: Total heat output for pre-combustion setup with and without CaL

The heat shown in Figure 3.11 has lower value compared to the post-combustion capture case.

Figure 3.12 shows the comparison of energy penalty between the post-combustion and pre-combustion cases. It can be observed that the pre-combustion capture generally has a higher energy penalty.

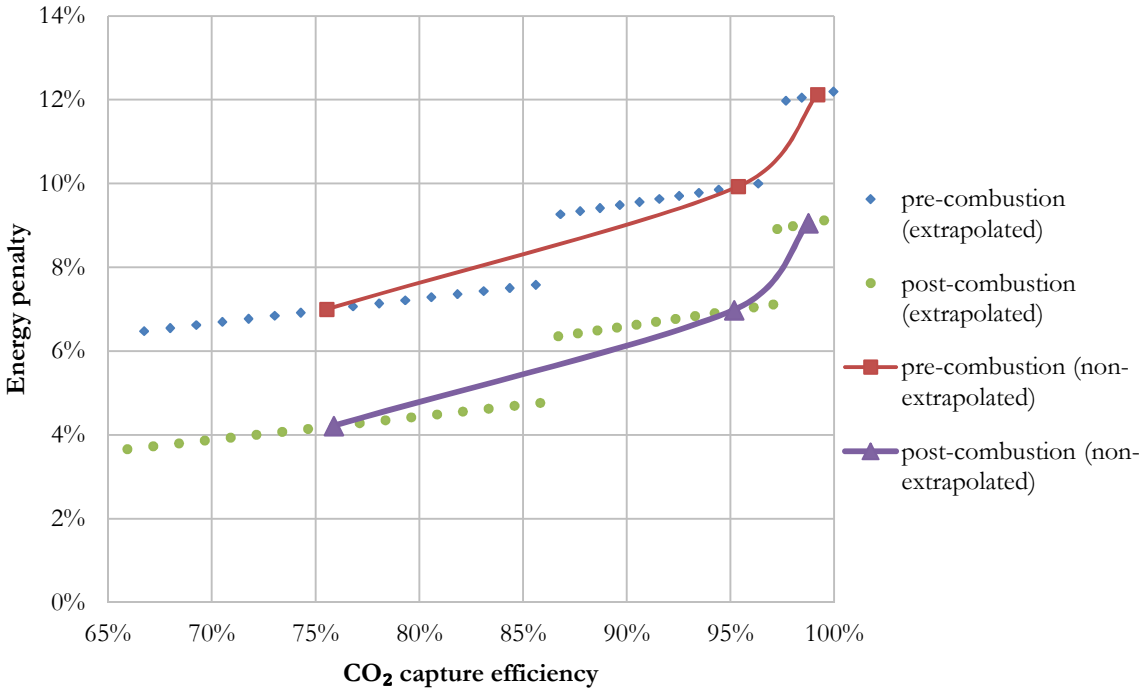

Figure 3.12: Energy penalty vs. CO_2 capture efficiency in pre-combustion capture

3.5 Scaling of Calculations

The original inflow rate of coal considered so far is 50 kg/s. In order to show the ability for the CaL model to produce accurate results by change of scale, another case with smaller coal inflow rate of 5 kg/s is calculated. For the down-scaled case, the heat outputs for the post-combustion and pre-combustion cases are shown in Figure 3.13. With smaller coal inflow rate the energy output in the pre-combustion case is smaller than that for the post-combustion case as expected. Figure 3.14 shows the comparison between the energy penalty in pre-combustion and post-combustion case for two different coal inflow rates.

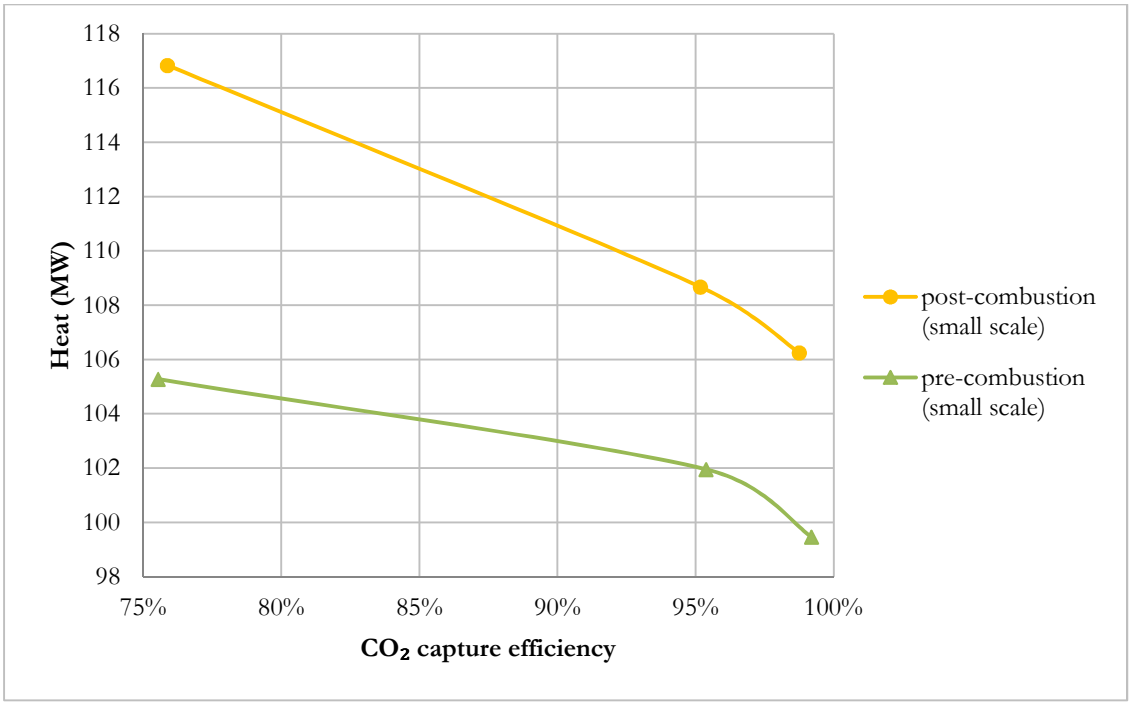

Figure 3.13: Comparison of heat output for post- & pre-combustion cases with smaller-scale coal inflow rate of 5 kg/s

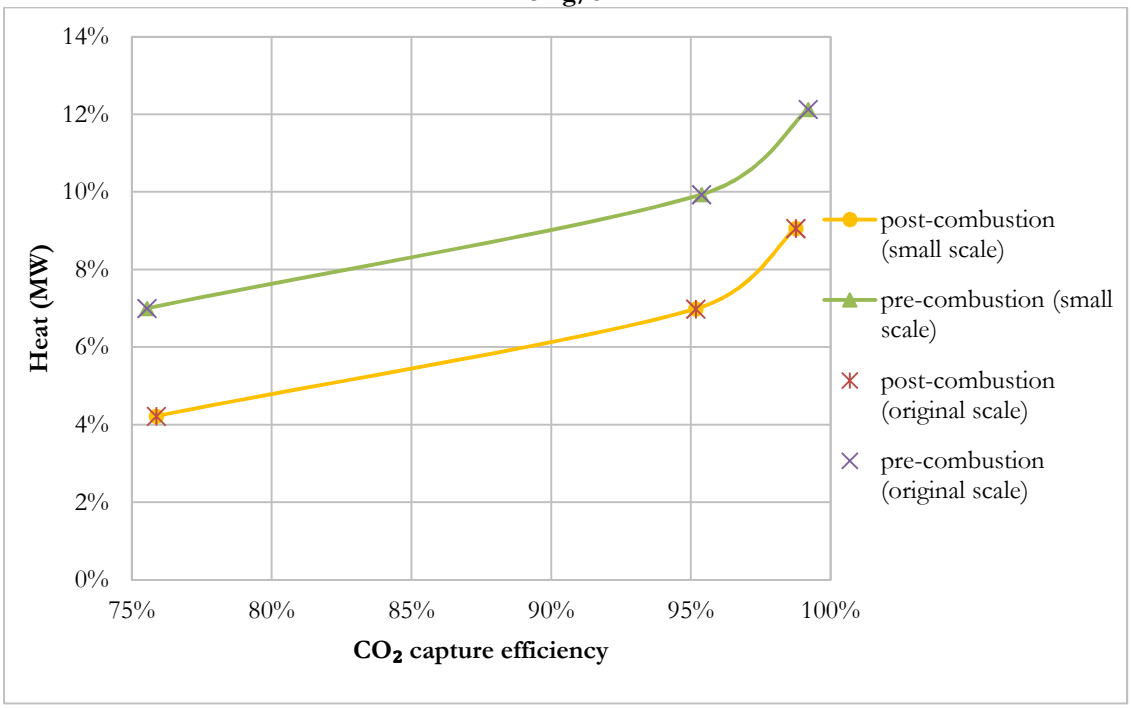

Figure 3.14: Comparison of energy penalty for post- and pre-combustion cases with the original scale (50 kg/s) and smaller scale (5 kg/s) coal inflow rate

It can be seen from Figure 3.14 that, different scaling does not affect the results for energy penalty.

3.6 Conclusions

It has been demonstrated that the energy penalty computed in CaL using ASPEN Plus for both the post-combustion and pre-combustion cases is basically related to the amount of CaO that comes into the carbonator. By setting the inlet and outlet temperatures for solid (CaO and $CaCO_3$) at 25 ºC and 150 ºC respectively, the amount of energy consumed for heating up the solid is the main source of energy penalty in CaL. When the CaO to CO_2 flow rate ratio increases, the energy consumption also increases for every energy unit amount of CO_2 captured.

Chapter 4 Reactor Level Simulations

4.1 Introduction

This CFD simulations presented in this chapter are not based on any actual laboratory scale or pilot scale reactor. The reactor model considered in this chapter has a simple shape of a cylinder. Reaction in a cylinder can be easily calculated using an axi-symmetric model. Due to plane of symmetry, it is sufficient to consider half cross-section of the cylinder. By using the plane of symmetry instead of the complete axi-symmetric model, the computational time in CFD simulations is approximately reduced by a factor of two. We employ both the half model and the full axi-symmetric model for the purpose of comparison of results. Figure 4.1 shows the dimensions of the cylindrical reactor.

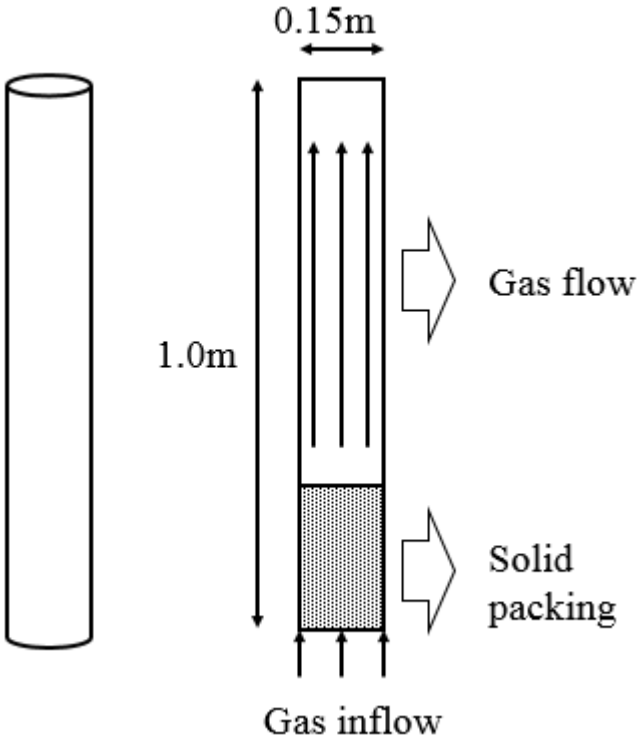

Figure 4.1: Carbonation fluidized bed reactor for CFD simulation (the axi-symmetric shape and its cross-section)

The species fractions in the inlet gas in the reactor is obtained from the results of ASPEN Plus calculations in the post-combustion case. The velocity of the inlet gas is chosen to be 0.25 m/s

which is suitable to create fluidization in this case. We will refer to the full axi-symmetric model setup as the original case. A total of four simulations are conducted by varying one of the following parameters: the half or full axi-symmetric model, the gas inlet velocity and the gas inlet CO_2 fraction. The differences between the four cases considered are summarized in Table 4.1.

Table 4.1: Setup for 4 cases in CFD simulation

	Case 1	Case 2	Case 3	Case 4
Name of case	Planar symmetry	Axial symmetry	Axial symmetry with reduced CO_2	Axial symmetry with reduced velocity
Type of model	Half symmetric	Axi-symmetric	Axi-symmetric	Axi-symmetric
Inlet CO_2 mole fraction	0.151	0.151	0.07	0.151
Inlet gas velocity (m/s)	0.25	0.25	0.25	0.125

4.2 Geometry and Mesh

This geometry of the half cross-section of the cylinder with dimensions is shown in Figure 4.2.

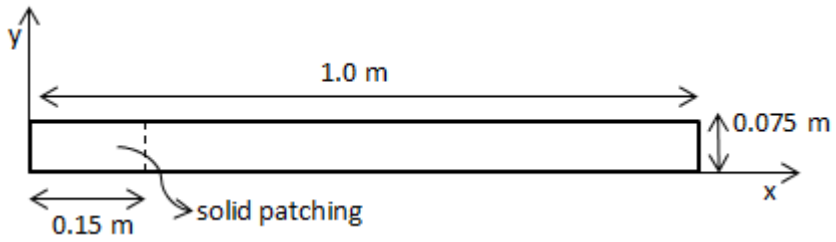

Figure 4.2: Geometry of the half cross-section of the reactor

In order to use the symmetry in the 2D model in FLUENT simulations, the geometry must use the x-axis as the axis of symmetry, so that the FLUENT can recognize it as the axis of symmetry.

Therefore the geometry of the reactor was rotated by 90°. For this orientation, the gravity must be set in the negative x direction in FLUENT. It is rotated back to its upright position when the results are presented.

The mesh in the reactor consists of structured square-shaped cells of uniform size as shown in Figure 4.3. The horizontal edge count is 14 and the vertical edge count is 198, with a total of 2772 cells. For the sake of showing the whole cross-section of the reactor, the other half part about the axis of symmetry has been added in Figure 4.3.

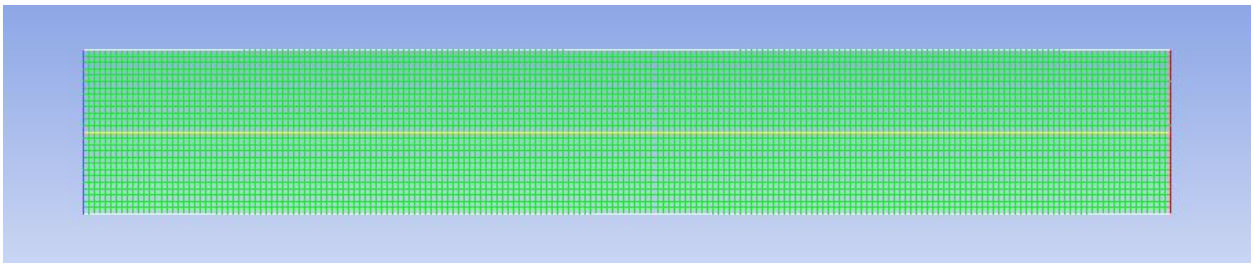

Figure 4.3: Mesh used in CFD simulations

4.3 Numerical Simulation Methodology

4.3.1 CFD Equations Solver

The commercial CFD solver ANSYS FLUENT is used in the simulations. The following selecionts are made in the solver.

- Pressure-based, transient solver is selected. The gravity is set at -9.81 m/s^2 on the x axis of the geometric model.

- The 2D model is set to be planar for planar case with symmetry. The 2D model is set to be axi-symmetric for axi-symmetric case.

- The Eulerian multi-phase model (granular flow model) is selected to handle the two phases as one fluid.

- The energy equation is employed.

- The flow is considered laminar.

- Species transport equations are employed to define the mixtures.

- A user defined function (UDF) is created for the drag law to model the interaction and momentum exchange between the solid and gas phases. The modified version of Syamlal-O'Brien's drag law (Syamlal and Obrien, 1989) is employed to create the UDF.

- For heat transfer, Gunn's heat transfer law (Gunn, 1978) is employed to enable the heat exchange between the two phases. If this law is not enabled, the heat produced by the chemical reaction will be solely transferred to the primary gaseous phase; it will heat up the gas phase and leave the temperature of the solid phase unchanged, which is not physical.

- There is only one reaction considered in the simulation; reactants include CO_2 from the gas phase and CaO from the solid phase, both of which have stoichiometric coefficient of 1 and rate exponent of 1. Product of reaction is $CaCO_3$, with stoichiometric coefficient of 1. The Arrhenius rate for reaction rate function is used. The constants used for Arrhenius rate are summarized Table 4.2 (Lee, 2004).

Table 4.2: Activation energy and pre-exponential factor for carbonation reaction (Lee, 2004)

	Chemical reaction control regime	Diffusion control regime
Activation energy (kJ/mol)	72.7	102.5
Pre-exponential factor (min^{-1})	1.16×10^4	2.33×10^5

4.3.2 Definition of Materials Considered in Simulation

Two mixtures are defined—the flue gas and the calcium solids. All components of these mixtures are directly copied from FLUENT materials library. The density option for each mixture is chosen to be the 'volume weighted mixing law'.

Flue gas consists of CO_2, H_2O, O_2, and N_2. The mole fractions are introduced from the inlet stream of carbonator in ASPEN Plus post-combustion simulation results. These fractions are defined in the boundary conditions.

Calcium solids consists of CaO and $CaCO_3$. CaO is the reactant for carbonation reaction, while $CaCO_3$ is the product of reaction. They both appear in the reaction. Thus they both need to be defined. In the two-phase flow, gas is to be the primary phase of the two Eulerian phases. The solid is set to be the secondary phase. Eulerian-Eulerian granular flow model is used for simulation of the single fluid behavior of two phases. Set diameter to be 0.0003 m. Syamlal-O'Brien drag law is chosen to define the granular viscosity.

4.3.3 Boundary and initial conditions

A summary of boundary conditions is shown in Figure 4.4. The left side of geometry in Figure 4.4 is the velocity inlet. For solid phase in the 'multiphase' flow, the volume fraction is set to be 0. For gas phase, the velocity is set to be 0.25 m/s (0.125 m/s for the reduced-velocity case) normal to boundary. For 'species', the mole fractions for CO_2, H_2O and O_2 are specified, leaving N_2 to be automatically determined. Values are given in Table 4.4 (for reduced CO_2 case) and Table 4.3 (all other cases).

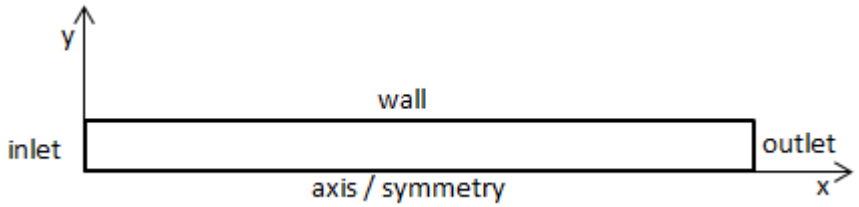

Figure 4.4: Boundary conditions for CFD simulation

Table 4.3: Inlet gas species mole fractions for the original case

CO_2	H_2O	O_2	N_2
0.151	0.081	0.019	0.749

Table 4.4: Inlet gas species mole fraction for the reduced-CO2 case

CO_2	H_2O	O_2	N_2
0.070	0.081	0.100	0.749

The right side of the geometry in Figure 4.4 is the pressure outlet with the gauge pressure = 0.

The top side of the geometry in Figure 4.4 is the wall. In order to simulate the reactor maintained at a certain temperature, the temperature of walls is set at 923 K. This temperature may cause the interior temperature to increase over 923 K, but the increase will not be too significant.

The bottom side of the geometry in Figure 4.4 is as an axis of symmetry for the planar case and an axis of rotation for the axi-symmetric case.

Initial conditions are summarized in Table 4.5.

Table 4.5: Initial conditions for CFD simulation

Variable name	Value
Gauge pressure (Pa)	0
Gas x & y (radial & axial) velocity (m/s)	0
Gas CO_2 fraction (within gas phase)	0
Gas H_2O fraction	0
Gas O_2 fraction	0
Gas temperature (K)	923 K
Solid x & y (radial & axial) velocity (m/s)	0
Solid volume fraction	0
Solid granular temperature (m^2/s^2)	0.0001
Solid CaO fraction (within solid phase)	1
Solid temperature (K)	923 K

After initializing with tabulated values in Table 4.5, we patch some solid at the bottom of the reactor. Patching region is shown in Figure 4.2. Patching with volume fraction of 0.55 is used. This patched volume fraction for solid acts as its initial condition.

4.3.4 Numerical Solver setup

The solution algorithms are summarized in Table 4.6. The under-relaxation factors used for various variables and equations are summarized in Table 4.7. Default simple solution methods are used except for the phase coupled method. Under-relaxation factors are used for adjusting the convergence of solution. These factors are the same as given in FLUENT tutorial guide (ANSYS, 2011).

Table 4.6: CFD solution algorithms used in FLUENT

Category	Option
Pressure-velocity coupling scheme	Phase coupled simple
Gradient spatial discretization	Least squares cell based
All other spatial discretization	First order upwind
Transient formulation	First order implicit

Table 4.7: Under-relaxation factors used for various variables and equations in FLUENT

Factor name	value
Pressure	0.5
Density	1
Body forces	1
Momentum	0.2
Volume fraction	0.4
Granular temperature	0.2
Energy	1
Mass for all species	1

Table 4.8 shows the transient settings in ANSYS FLUENT.

Table 4.8: Transient settings CFD solver FLUENT

Variable	Value
Time step size	0.001 s (0.0005 s for axi-symmetric case)
Number of time steps	10000 - 30000
Iterations per time step	20

Planar symmetry case has a time step size of 0.001s. Axi-symmetric case has a smaller time step size of 0.0005s, while the other two cases using the axi-symmetric model have time step of 0.001s. The number of time steps of 10000 is equivalent to a flow simulation time of 10 seconds. Some cases have been run for 15 seconds. For axi-symmetric case, 30000 steps are needed for 15 seconds of actual flow simulation time.

4.3.5 Numerical Data Collection

In conducting the calculations, we auto save the solution every 100 time steps. This saves the data files that contain information about the flow field, including the contours and vector plots of various flow variables etc.

In order to record the CO_2 mole fraction at the outlet, a surface monitor is created and an area-weighted average and mole fraction of CO_2, on the surface of 'outlet' is chosen. The data is plotted to a window. The data is collected at every 10 time steps and is written to the data file.

The total mass of solid is monitored to indicate the progress of reaction, since solid mass increases when CaO gradually turns into $CaCO_3$; the increased mass is identical to the captured mass of CO_2. In order to record the total mass of solid, a volume monitor is created which monitors the mass of the solid phase, while other settings stay the same.

4.4 Results

4.4.1 Contours and Vector Plots of Various Flow Quantities

All axi-symmetric cases tend to reach a steady state in solid volume fraction. Figure 4.5 shows contours of volume fraction and velocity vectors of solid phase for original case at flow time of 15s. The original case achieves steady state after about 1.7 seconds. The contours and vectors in Figure 4.5 remain unchanged after 1.7 seconds.

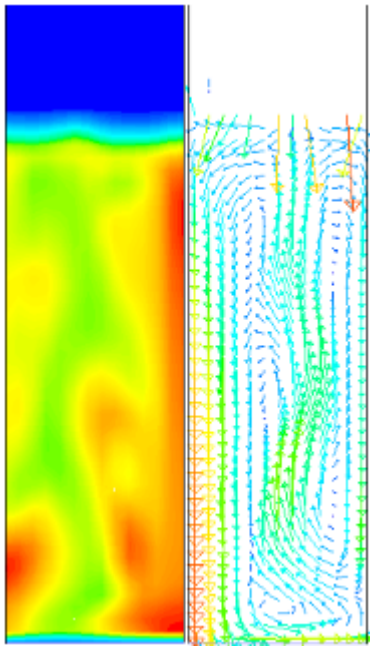

Figure 4.5: Volume fraction contours (left) and velocity vectors (right) of solid phase in axi-symmetric case at 15s (steady state is achieved in nearly 1.7 seconds)

Not all cases were run up to 15s; majority of cases were up to 10s. The volume fractions of solid phase at flow time of 10s are shown for planer and axi-symmetric case in Figure 4.6.

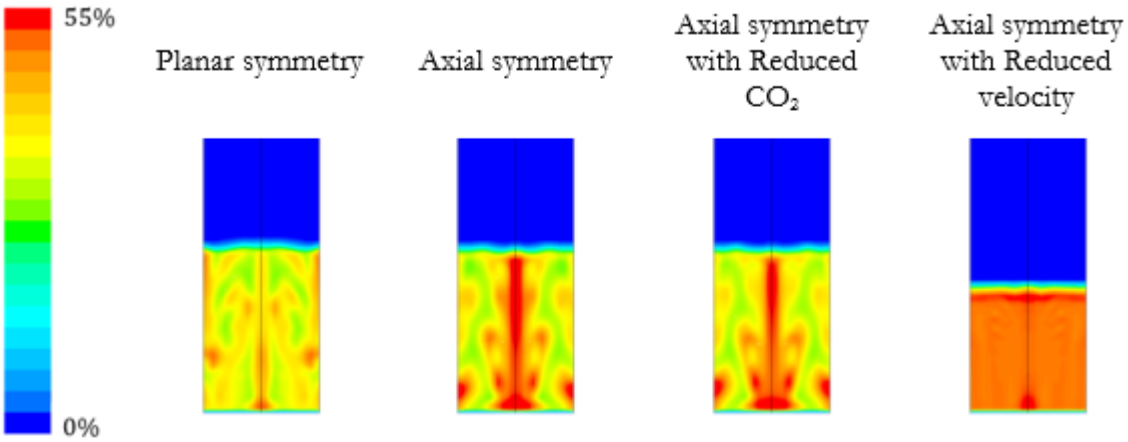

Figure 4.6: Solid volume fraction contours for multiple cases at 10s

One can see from Figure 4.6, all the cases have a fairly nice mixing and symmetry at steady when the flow becomes fully developed, and the solid phase becomes evenly distributed. The original case and the reduced-CO_2 case with axial symmetry are basically the same. Thus, in axi-symmetric model, the mole fraction of CO_2 in the inlet gas and how fast the reaction takes place do not have much effect on how the distribution of solid phase. However at reduced velocity, although having a fairly even distribution of solid, fluidization hardly develops.

Figure 4.7 shows the vectors at 10s of flow time. It can be seen that in all cases, there is a region in the middle of the reactor where the entire solid phase is moving downward. This is quite different than what would be generally expected. Due to no-slip wall boundary condition friction causes gas to rise at a slower velocity near the wall than away from wall. Thus, when the gas flow forces solid to circulate, it is reasonable to assume that the solid would go up in the region where gas rises faster (that is in the middle) and will go down where the gas rises slower (near the wall). But this conclusion is opposite to the simulation result in the middle region of the reactor. Closer observation of simulations reveals that the region for upward movement solid is actually a region between the wall and the axis. Also, the planar symmetric case has a narrower region in the middle for downward flow of solids.

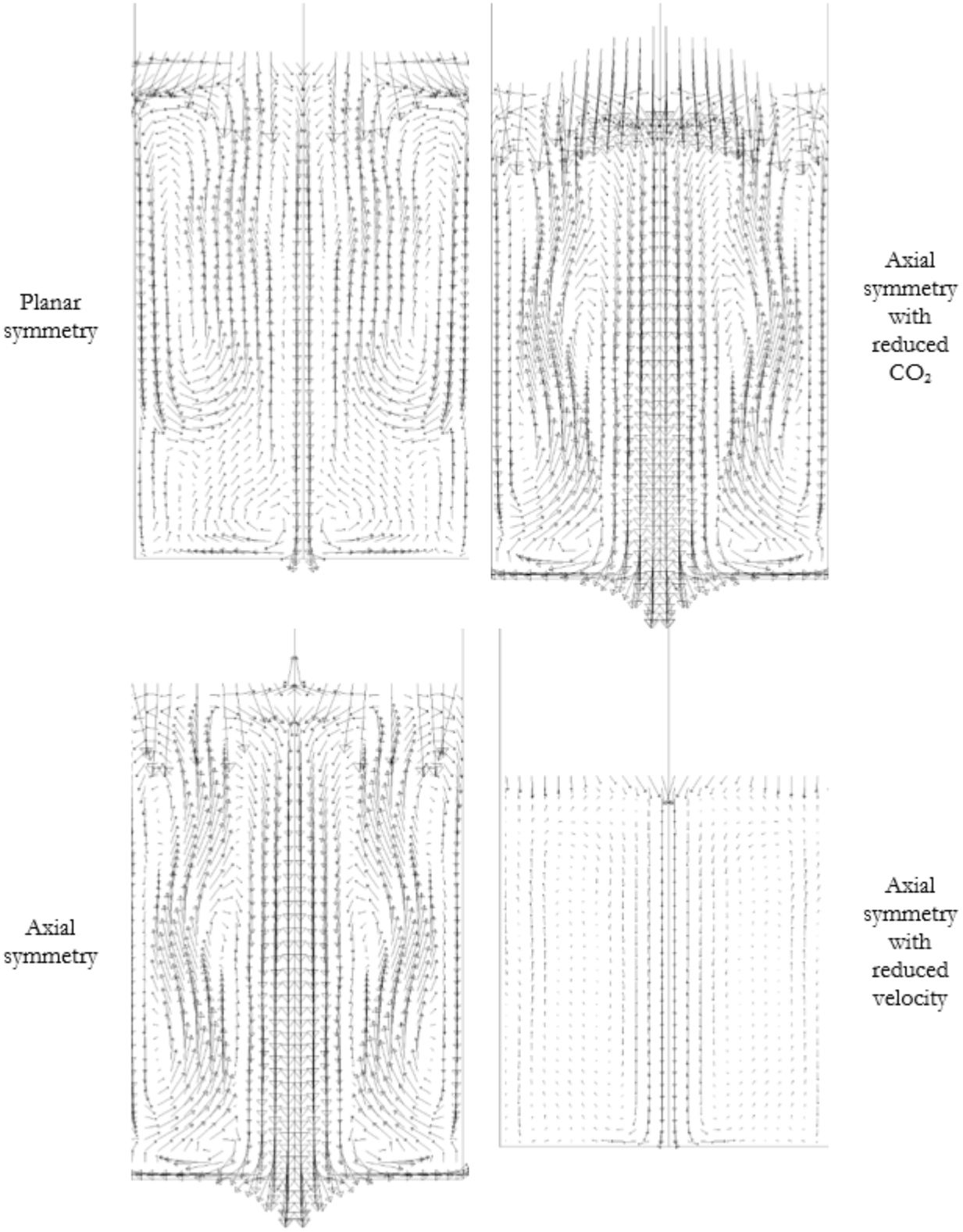

Figure 4.7: Velocity vectors for four different cases of Figure 4.6 at 10s

One can see difference in circulation inside the reactor for planar symmetric and axi-symmetric case. The planar symmetric case tends to have more circulation with circulation splitting into upper zone and lower zone. The velocity vectors for the axi-symmetric case look more like a spout bed. The original case and the reduced CO_2 case appear to have the same pattern for velocity vectors. However, the reduced velocity case hardly has any solid velocity.

Next, we consider the carbonation reaction. Figure 4.8 shows the mole fractions of $CaCO_3$ at three different time for the four cases of Figure 4.6.

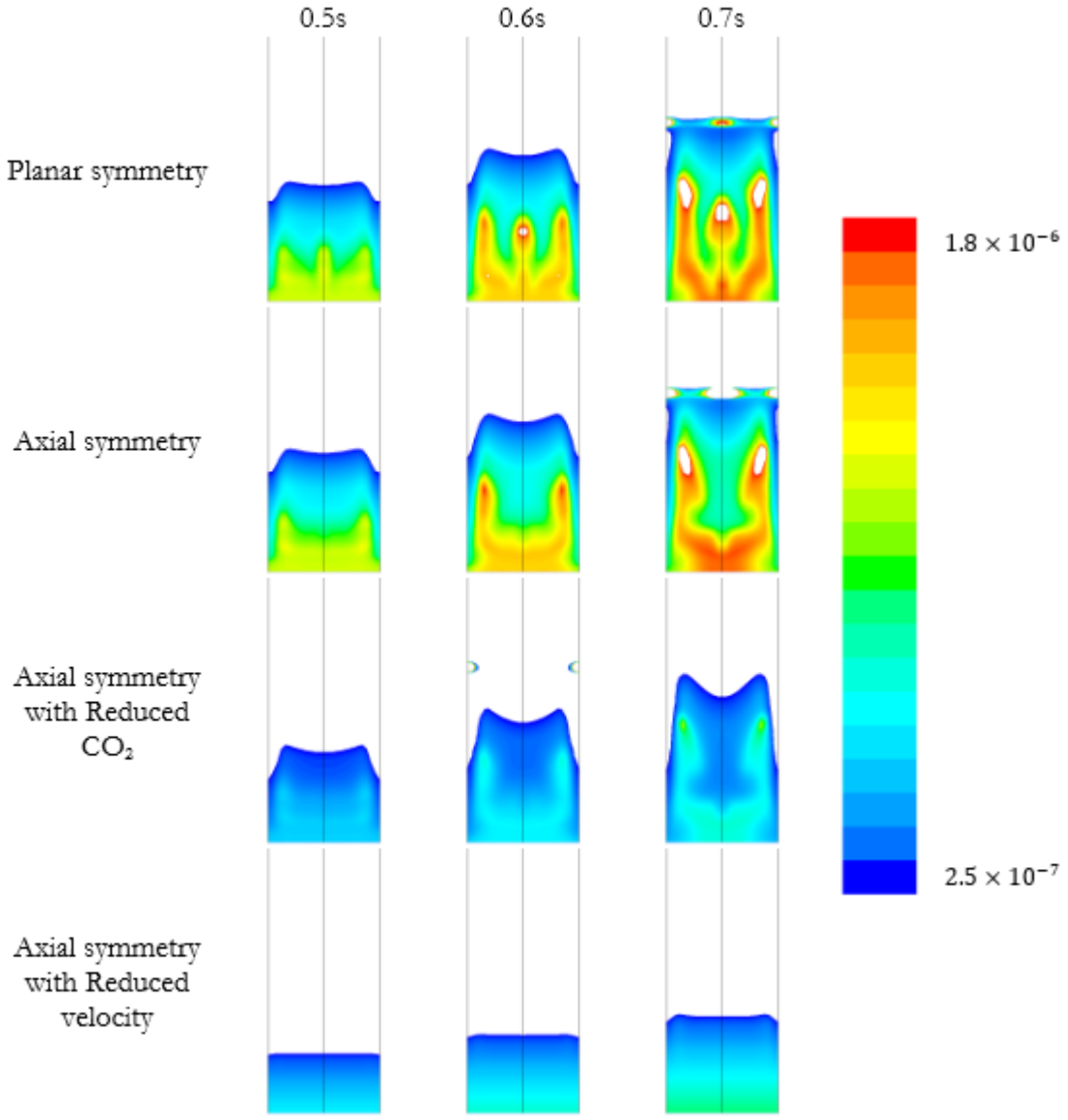

Figure 4.8: CaCO3 mole fraction contours for multiple cases and flow time

From Figure 4.8, one can note the origination and migration of $CaCO_3$. For the original case, the $CaCO_3$ forms at the bottom of the reactor, and begins to migrate upward, with the middle region migrating at a lower speed and even stopping at some point. The region close to the wall faster migration. Relating this behavior to the velocity vectors of the solid flow, they agree well with each other, in the sense that the flow in the middle region is going downward and is upward in the region close to the wall. The highly-concentrated $CaCO_3$ region coincides with the upward movement

region of the solid flow. This is due to lower density of $CaCO_3$ compared to CaO; therefore the region where $CaCO_3$ fraction is higher tends to be more easily driven by the gas.

Comparing the planar symmetric case with the axi-symmetric case, the most obvious difference is that the planar symmetric case has a middle region of highly concentrated $CaCO_3$, which may be due to the fact that the planar symmetric case has a narrower region for solid phase in the middle to go downward. Thus, whether the solid goes up or down in the reactor seems to have relation with the $CaCO_3$ mole fraction.

The reason that the period from 0.5s – 0.7s is chosen is that, after this period, $CaCO_3$ tends to form a high fraction zone in the top of the fluidization region. This fraction is so high that the region of interest (where solid is closer to the inlet) can hardly be displayed. Some $CaCO_3$ particles appear to eject to form high $CaCO_3$ fraction (10^{-2}compared to previously10^{-6}) areas. This phenomenon can be explained by the lower density of $CaCO_3$; however this unusually high fraction is not of interest in this thesis. After narrowing down the range of display around 10^{-4}, the bottom region of the reactor begins to show evenly distributed $CaCO_3$.

The reduced-CO_2 case has the same shape as the original case but with lower values. The reduced-velocity case almost has a horizontal-layer distribution, which is similar to the other cases at earlier time steps.

4.4.2 Reaction Rate Analysis

In carbonation reaction, solid mass increases when CaO changes to $CaCO_3$; the difference in the mass of CaO and $CaCO_3$ is the mass of CO_2. To derive the reaction rate of CO_2, we need to monitor the change in solid mass as shown in Figure 4.9. The increase in solid mass can indicate how much CO_2 has reacted, which can provide the reaction rate. Since the absolute increment amount of $CaCO_3$ is too small, we consider the ratio of increased mass to the original mass, calling it proportional increment and use ppm instead of percentage increase for display.

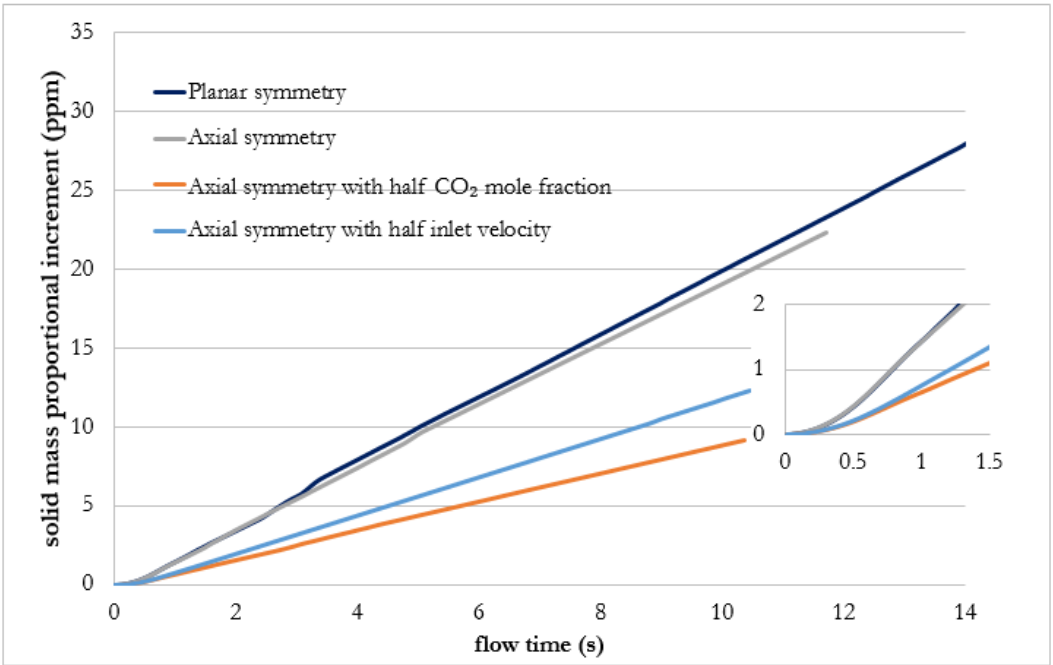

Figure 4.9: Proportional increment in solid mass with time for four cases of Figure 4.6

With this relation between the increased solid mass and the reacted CO_2 mass, one can get the mass of CO_2 that has reacted during a small time period of 0.005s or 0.01s. Divide it by 44 to get the number of moles of CO_2, and then divide it by time duration, and finally divide it by the volume of the packing region to obtain the bulk reaction rate of CO_2 within the packing region. By this calculation, the unit for reaction rate becomes mol/m^3/s. The height of the packing region is assumed to be 0.2 m, which is higher than the initial packing of 0.15 m, to account for the fluidization. Figure 4.10 shows comparisons of the CO_2 reaction rate for the four cases of Figure 4.6.

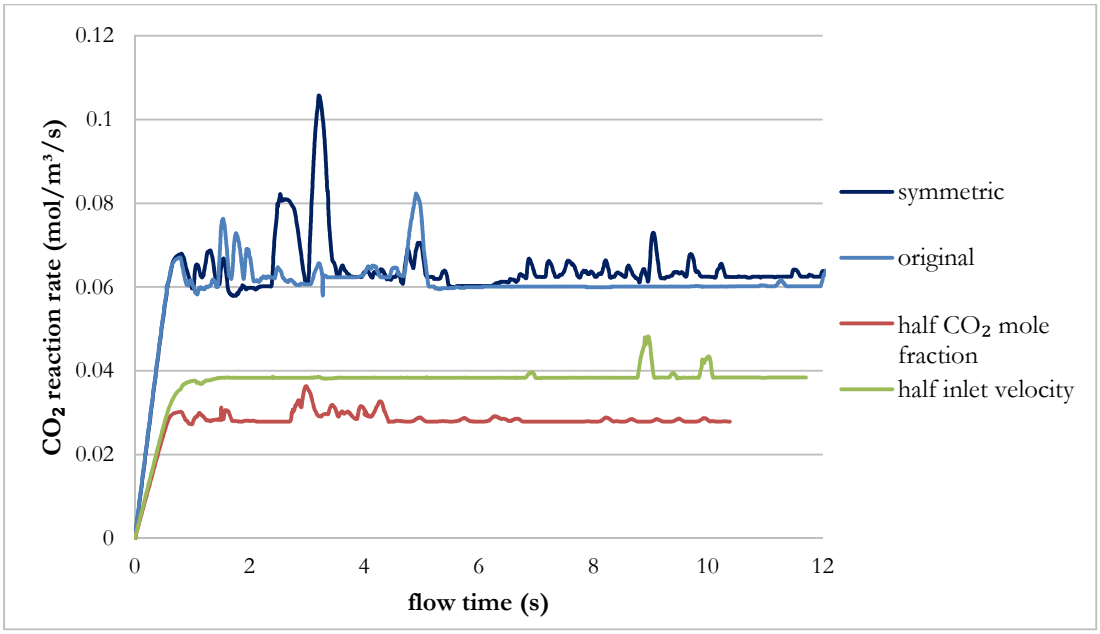

Figure 4.10: CO2 reaction rate vs. flow time for the four cases of Figure 4.6

Initially, the reaction rate increases, then maintain a relatively stable rate (except for some fluctuations). In the stable region, the reduced-CO_2 case has nearly half the reaction rate of original case, while the reduced-velocity case has more than half of the reaction rate of original case. From the model setup, reduced-CO_2 case has half of the CO_2 inlet fraction; and the reduced-velocity case has half of the inlet velocity. Thus the results indicate that, by decreasing the inlet CO_2 mole fraction, its reaction rate decreases proportionally, while by decreasing the velocity, reaction rate decreases less than proportionally. Therefore, one can conclude that with lower velocity, the gas molecules have more chance to react with the solid and thus they are better mixed. In summary, a higher concentration and reasonably lower velocity may contribute to higher reaction rate for CO_2 in carbonation.

For comparison between the planar symmetric and axi-symmetric models, they agree well in the early rising region. Although with large fluctuations, they nevertheless match with each other. These fluctuations may have something to do with the mixing conditions, since the way solid distributes itself is constantly changing.

4.4.3 CO_2 Capture Efficiency Analysis

To derive the CO_2 capture efficiency, one needs to monitor the mole fraction of CO_2 at the outlet shown in Figure 4.11. This provides information when the gas flow reaches the outlet and how much CO_2 stays in the reactor.

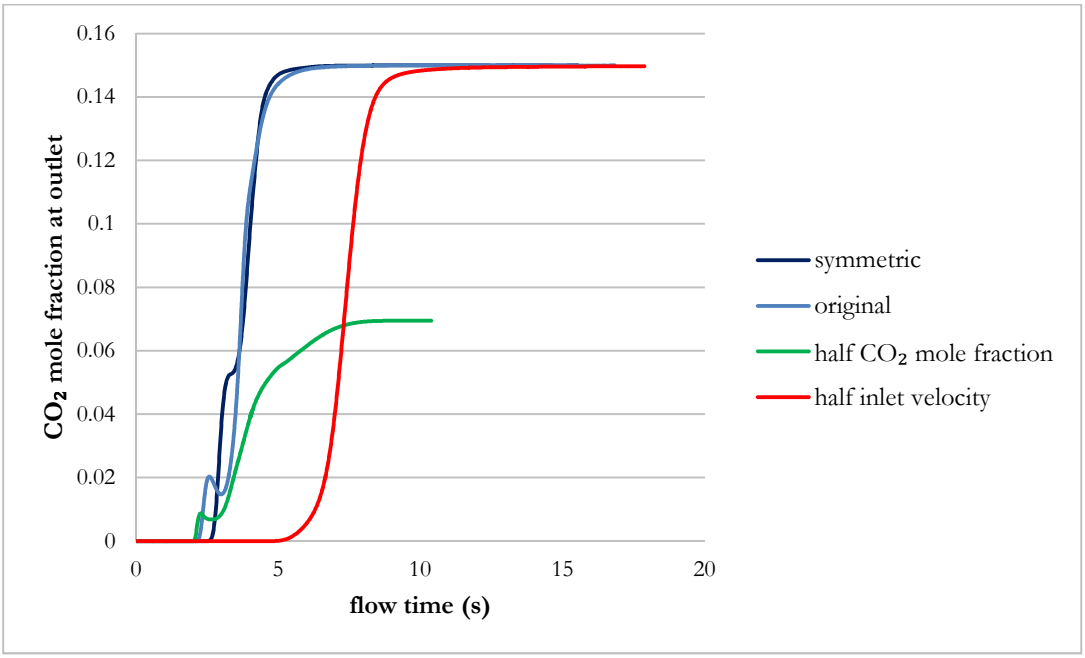

Figure 4.11: Outlet CO2 mole fraction vs. flow time for four cases of Figure 4.6

To calculate the CO_2 capture efficiency, some algebraic manipulations are required. This calculation is accurate without any approximation. Result is shown in Figure 4.12. In order to have a closer look where they may differ in the stable region, a logarithmic plot is used to zoom-into the values around 1 %.

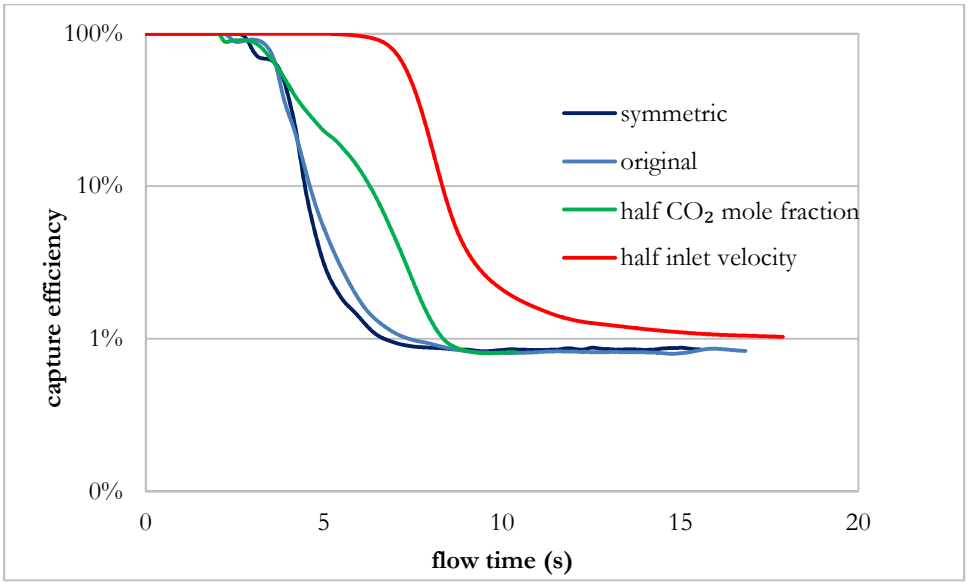

Figure 4.12: CO2 capture efficiency vs flow time for four cases of Figure 4.6

The low-capture-efficiency result is not ideal, which may be due to the geometry of the reactor or by not choosing the correct pre-exponential factor. Besides that, nevertheless there is something to compare among the four cases. One can observe that at least 3 cases finally merge to the same value of CO_2 capture efficiency. Whether it will merge remains uncertain for the reduced-velocity case, since the curve is left in instability region due to constrains on the calculation time. What can be deduced from Figure 4.12 is that with lower inlet CO_2 mole fraction, the CO_2 capture efficiency will not change.

Furthermore, Figure 4.12 also shows how well the curves from planar symmetric case and the original axi-symmetric case overlap with each other.

Chapter 5 Conclusions

An energy penalty calculation for post-combustion and pre-combustion Calcium looping (CaL) process is carried out using ASPEN Plus in. Flow sheets for post-combustion and pre-combustion CO_2 capture models are developed. To achieve a capture efficiency of 50 – 99%, energy penalty for post-combustion capture is in the range 4 – 10%; for pre-combustion capture it is in the range 6 – 12%. For high capture of CO_2 (above 90%), the marginal energy penalty increases dramatically as the capture efficiency increases. Thus, 99% CO_2 capture may be a desirable limit, however the Calcium looping may become impractical due to energy consumption. The models developed in this thesis can be scaled for higher and lower flow rates of coal input.

A CFD simulation in a CaL reactor is conducted using the CFD software ANSYS FLUENT. A planar symmetric and an axi-symmetric model of the reactor are considered. Different inflow-gas conditions are considered. Planar Symmetric model and the axi-symmetric model differ a great lot with respect to the results concerning solid distribution in the reactor. However, they give nearly the same results regarding the overall progress of the chemical reaction. Furthermore, for the inlet-gas condition, higher CO_2 fraction and lower velocity are found to contribute to better progress in chemical reaction.

References

[1] Abanades, J.C., Anthony, E.J., Wang, J., and Oakey, J.E., "Fluidized Bed Combustion Systems Integrating CO_2 Capture with CaO," *Environ. Sci. Technol.* 39 (2005) 2861 – 2866.

[2] ANSYS, Inc., FLUENT Tutorial Guide, 2011.

[3] Cormos, C.-C. and Petrescu, L., "Evaluation of Calcium Looping as Carbon Capture Option for Combustion and Gasification Power Plants," *Energy Procedia* 51 (2014) 154 – 160.

[4] Feron P., "Post-Combustion Capture (PCC) R&D at CSIRO," COAL21 Post Combustion CO_2 Capture Meeting, 2008.

[5] Gunn, D.J., "Transfer of Heat or Mass to Particles in Fixed and Fluidized Beds," Int. J. *Heat Mass Transfer* 21 (1978) 467–476.

[6] Lee, D.K, "An Apparent Kinetic Model for the Carbonation of Calcium Oxide by Carbon Dioxide," *Chemical Engineering Journal* 100 (2004) 71 – 77.

[7] Marhalatkar, K., Kuhlmaj, J., Huckaby, E.D., and O'Brien, T., "CFD Simulation of a Chemical-Looping Fuel Reactor Utilizing Solid Fuel," *Chemical Engineering Science* 66 (2011) 3617 – 3627.

[8] Sivalingam, S., "CO_2 Separation by Calcium Looping from Full and Partial Oxidation Processes," PhD Dissertation, Technische Universität München, 2013.

[9] Syamlal, M. and O'Brien, T.J., "Computer Simulation of Bubbles in a Fluidized Bed,"*AIChE Symp* Series 85 (1989) 22–31.

Vita

Wei Dai

Degrees M.S. Mechanical Engineering, August 2015
B.S. Mechanical Engineering, June 2013

August 2015